

1970

Sedimentology of the Willwood Formation (Lower Eocene): an alluvial molasse facies in northwestern Wyoming, USA

John West Neasham
Iowa State University

Follow this and additional works at: <https://lib.dr.iastate.edu/rtd>



Part of the [Geology Commons](#)

Recommended Citation

Neasham, John West, "Sedimentology of the Willwood Formation (Lower Eocene): an alluvial molasse facies in northwestern Wyoming, USA " (1970). *Retrospective Theses and Dissertations*. 4255.
<https://lib.dr.iastate.edu/rtd/4255>

This Dissertation is brought to you for free and open access by the Iowa State University Capstones, Theses and Dissertations at Iowa State University Digital Repository. It has been accepted for inclusion in Retrospective Theses and Dissertations by an authorized administrator of Iowa State University Digital Repository. For more information, please contact digirep@iastate.edu.

70-25,812

NEASHAM, John West, 1941-
SEDIMENTOLOGY OF THE WILLWOOD FORMATION
(LOWER EOCENE): AN ALLUVIAL MOLASSE
FACIES IN NORTHWESTERN WYOMING, U.S.A.

Iowa State University, Ph.D., 1970
Geology

University Microfilms, A XEROX Company, Ann Arbor, Michigan

SEDIMENTOLOGY OF THE WILLWOOD FORMATION (LOWER EOCENE):
AN ALLUVIAL MOLASSE FACIES IN NORTHWESTERN
WYOMING, U.S.A.

by

John West Neasham

A Dissertation Submitted to the
Graduate Faculty in Partial Fulfillment of
The Requirements for the Degree of
DOCTOR OF PHILOSOPHY

Major Subject: Geology

Approved:

Signature was redacted for privacy.

In Charge of Major Work

Signature was redacted for privacy.

Head of Major Department

Signature was redacted for privacy.

Dean of Graduate College

Iowa State University
Of Science and Technology
Ames, Iowa

1970

TABLE OF CONTENTS

	Page
INTRODUCTION	1
REVIEW OF PREVIOUS WORK	4
REGIONAL STRATIGRAPHY	7
Stratigraphic Relationships and Thickness	7
Lithologic Facies	10
Conglomerate facies	10
Sandstone and mudstone facies	15
PETROLOGY	22
Conglomerates	22
Sandstones	25
Mineral composition	25
Texture	34
Mudstones	39
Mineralogy	39
Texture	45
Chemical constituents	50
SEDIMENTARY STRUCTURES	57
Simple Structures	57
Large-scale cross-stratification	58
Small-scale cross-stratification	61
Horizontal stratification	62
Composite Structures	62
Alluvial fan deposits	62
Channel deposits	64
Transitional deposits	64
Overbank deposits	68
Paleocurrent Data	69
DISCUSSION AND INTERPRETATION	74

	Page
Provenance	74
Composition	74
<u>In situ</u> alteration	76
Basin of Deposition	80
Depositional Patterns	86
CONCLUSIONS	89
ACKNOWLEDGEMENTS	91
REFERENCES CITED	93

LIST OF FIGURES

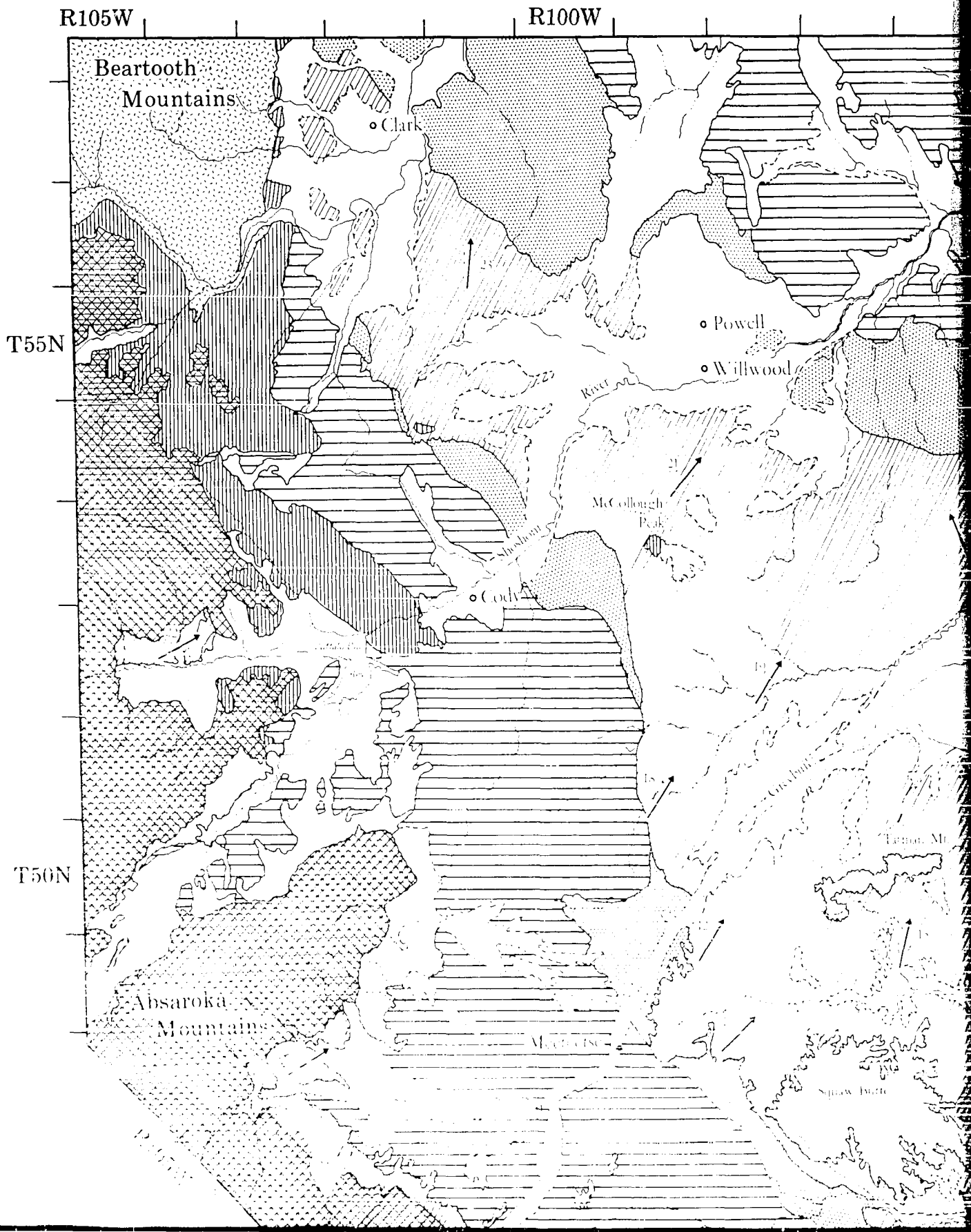
	Page
Fig. 1. Geologic map of the Big Horn Basin.....	3
Fig. 2. Development of terminology.....	6
Fig. 3. Graphic sections of the Willwood Formation in the central portion of the Big Horn Basin.....	9
Fig. 4. Photographs of Willwood lithologic facies.....	12
Fig. 5. Graphic section of Willwood conglomerates exposed near the town of Meeteetse.....	14
Fig. 6. Graphic sections of the Willwood along the Beartooth Mountain front.....	17
Fig. 7. Vertical lithic transitions of sandstone- mudstone facies derived from Markov chain analysis.....	20
Fig. 8. Percentages of grains, matrix, cement, and mineralogical components of Willwood sand- stones.....	27
Fig. 9. Textural and compositional classification of sandstones.....	29
Fig. 10. Heavy mineral frequencies.....	33
Fig. 11. Statistical measure values of sandstones.....	36
Fig. 12. Standard deviation verses mean size in sandstones.....	38
Fig. 13. Flow chart for X-ray analysis of mudstones.....	42
Fig. 14. Typical X-ray diffractometer tracing for Willwood mudstones.....	44
Fig. 15. Percentages of mineralogical components of Willwood mudstones.....	47
Fig. 16. Total and clay mineralogy of Willwood mud- stones.....	49
Fig. 17. Quantitative data on organic carbon and free iron, aluminium, and manganese in Willwood mudstones.....	52

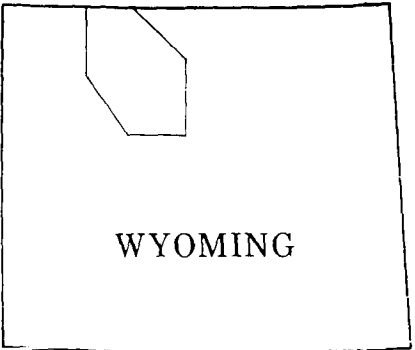
	Page
Fig. 18. Vertical distribution of clay, organic and inorganic carbon, free iron, aluminium, and manganese in Willwood mudstone sequence.....	55
Fig. 19. Photographs of simple and organic structures...	60
Fig. 20. Photographs of composite structures.....	66
Fig. 21. Paleocurrent data.....	72

INTRODUCTION

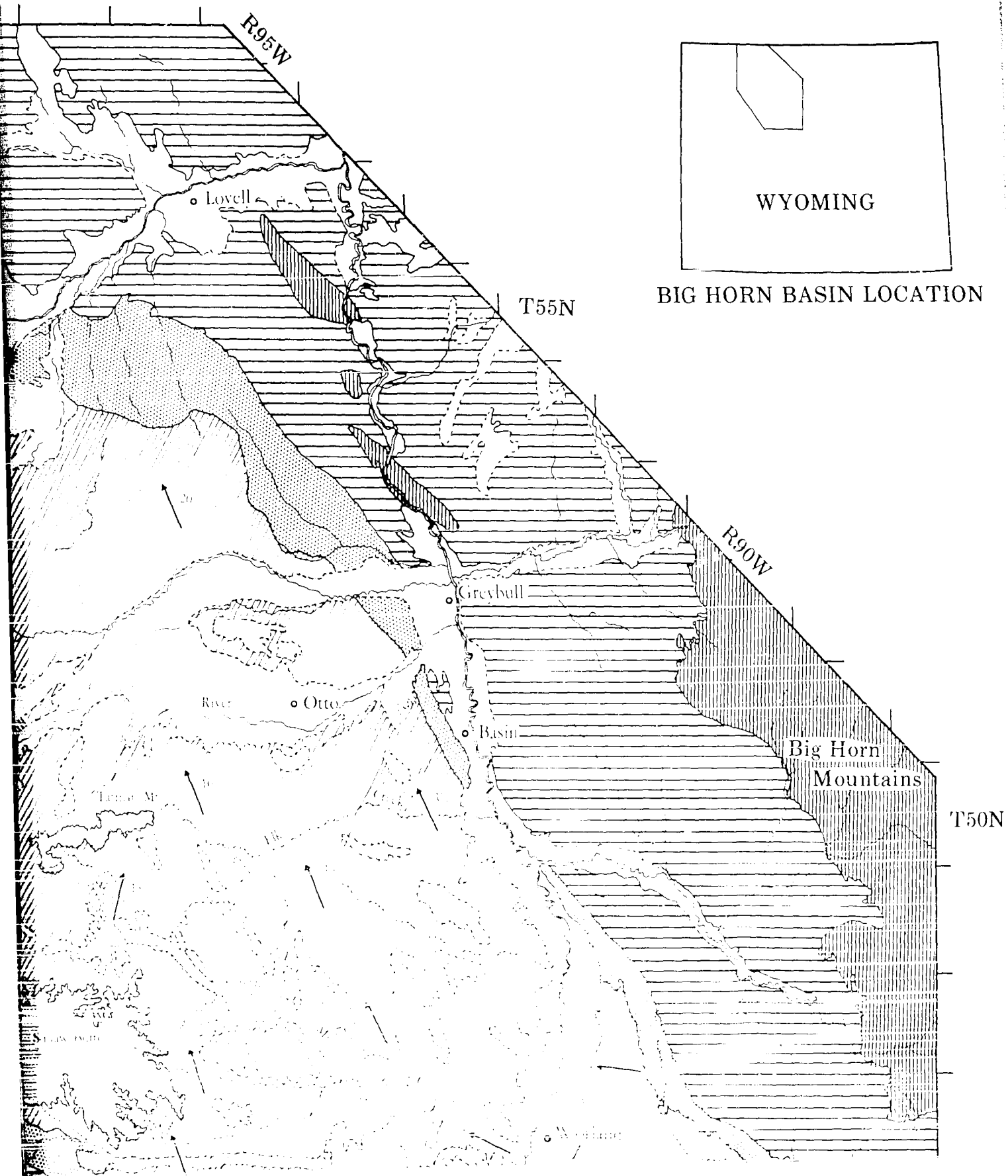
This report presents a detailed examination of the Willwood Formation, late Paleocene (Clarkforkian) to early Eocene (Wasatchian), in the Big Horn Basin in northwestern Wyoming (Fig. 1) and the synthesis of the information derived to provide a better understanding of its depositional history. Investigations of the Willwood and other red-banded, early Cenozoic deposits in the intermontane basins of the western United States date back approximately 100 years. Early studies were primarily directed toward the rich assemblage of mammalian remains preserved in these deposits. In more recent years, however, the lithologic and stratigraphic nature of the Willwood has received considerable attention.

FIG. 1 Geologic map of the Big Horn Basin.

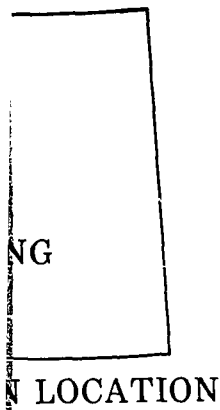




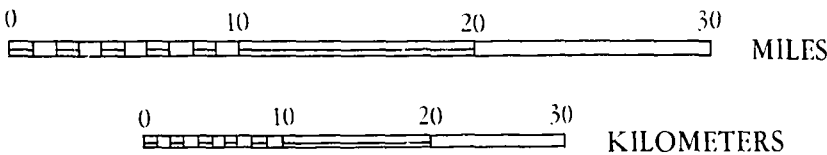
BIG HORN BASIN LOCATION



GEOLOGIC MAP OF THE BIG HORN BASIN, WYOMING



SCALE 1:500,000



EXPLANATION



Quaternary deposits

Unconsolidated or poorly consolidated gravel, sand, silt, and clay on floodplains, fans, and terraces; also loose rock debris and talus of landslide origin and glacial boulders, gravel, and sand along mountain fronts.



Polcat Bench Formation

Interbedded sandstones and drab mudstones; lignite and coal beds, occasional quartzite pebble conglomerates.



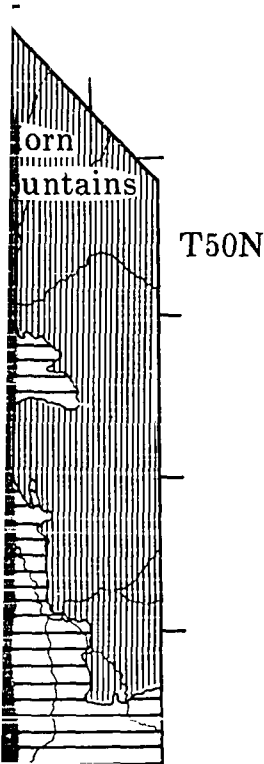
Middle and late Tertiary lava flows, breccias, and pyroclastic rocks

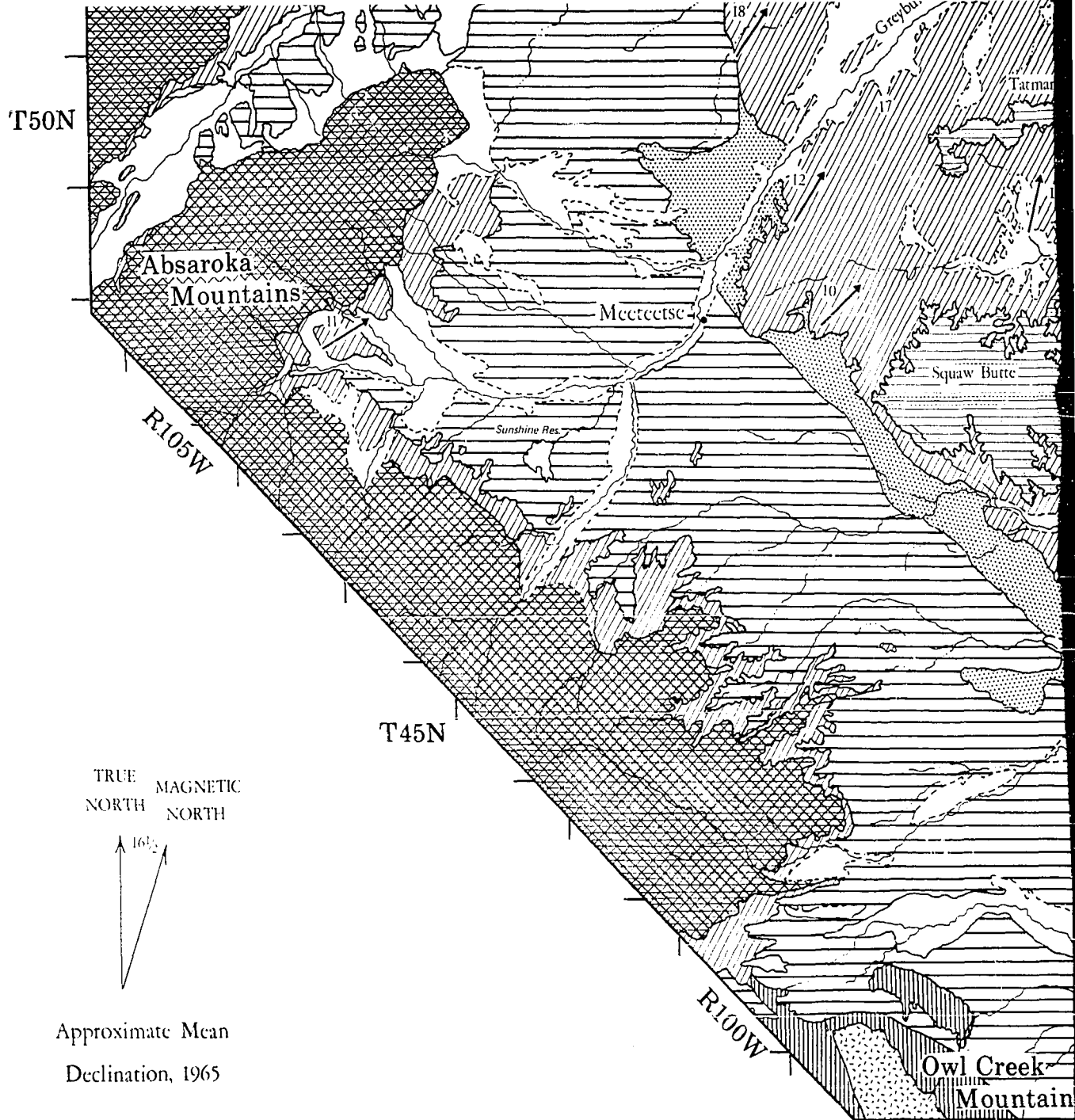
Acid and basic breccia, basalt flows, and minor areas of intrusive and extrusive igneous rock; also occasional volcanic conglomerates and andesitic conglomerate, sandstone, and mudstone.



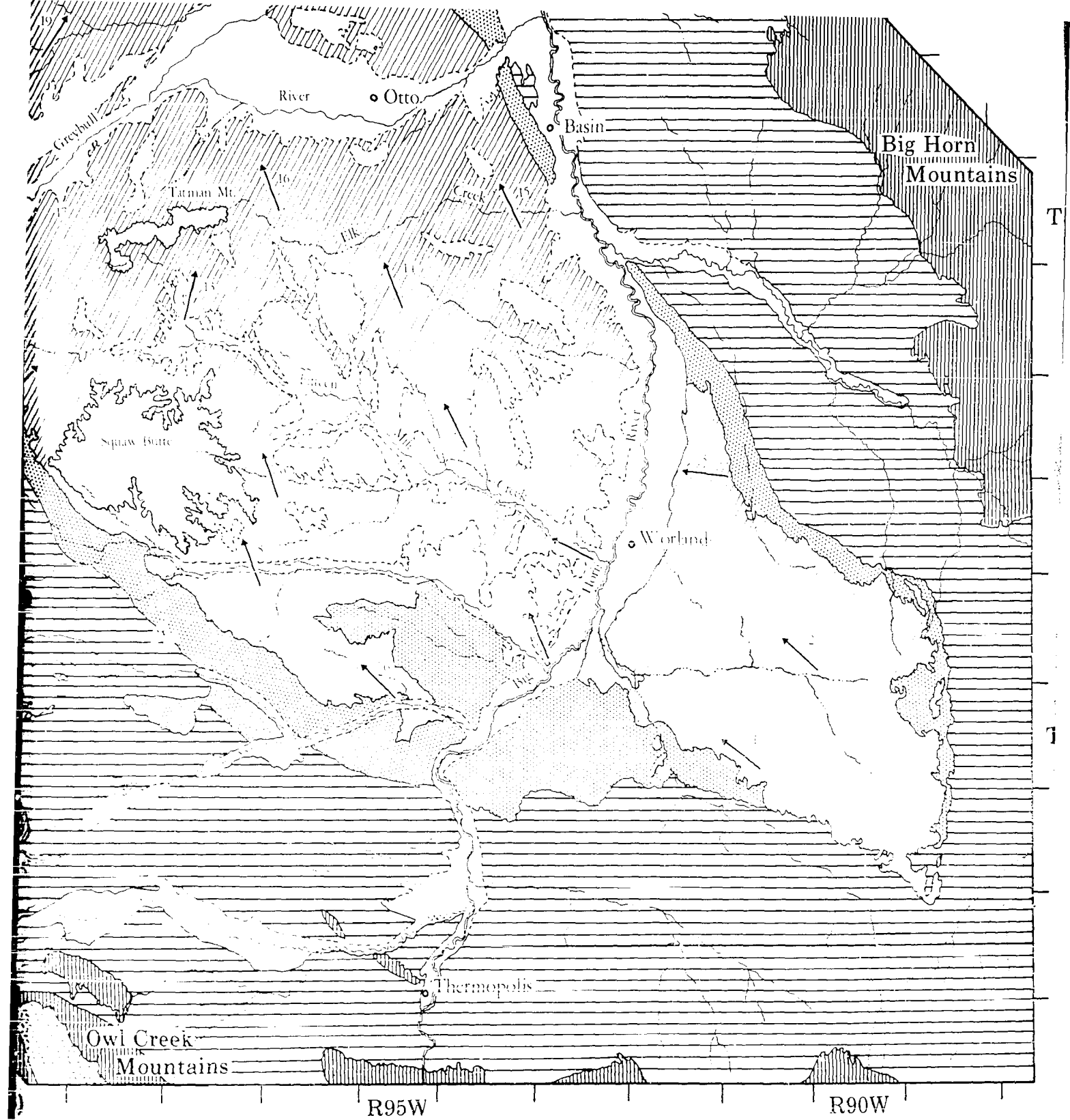
Mesozoic rocks, undivided

Basically sandstones and mudstones, includes (from oldest to youngest) Dinwoody, Chugwater, Gypsum Springs, Sundance, Morrison, Cloverly, Sikes Mt., Muddy, Mowry, Frontier, Cody, Mesaverde, Meetcote, and Lance Formations.





After GEOLOGIC MAP OF WYOMING (1955)





Quaternary deposits

Unconsolidated or poorly consolidated gravel, sand, silt, and clay on floodplains, fans, and terraces; also loose rock debris and talus of landslide origin and glacial boulders, gravel, and sand along mountain fronts.



Polecat Bench Formation

Interbedded sandstones and drab mudstones; lignite and coal beds; occasional quartzite pebble conglomerates.



Middle and late Tertiary lava flows, breccias, and pyroclastic rocks

Acid and basic breccia, basalt flows, and minor areas of intrusive and extrusive igneous rock; also occasional volcanic conglomerates and andesitic conglomerate, sandstone, and mudstone.



Mesozoic rocks, undivided

Basically sandstones and mudstones; includes (from oldest to youngest) Dinwoody, Chugwater, Gypsum Springs, Sundance, Morrison, Cloverly, Sykes Mt., Muddy, Mowry, Frontier, Cody, Mesaverde, Monteville, and Lance Formations.



Tatman Formation

Sandstone, drab mudstone and oil shale, lignite, and fresh-water limestone.



Paleozoic rocks, undivided

Basically carbonates and sandstones; includes (from oldest to youngest) Flathead, Gros Ventre, Gallatin, Big Horn, Madison, Amsden, Tensleep, and Phosphoria Formations.



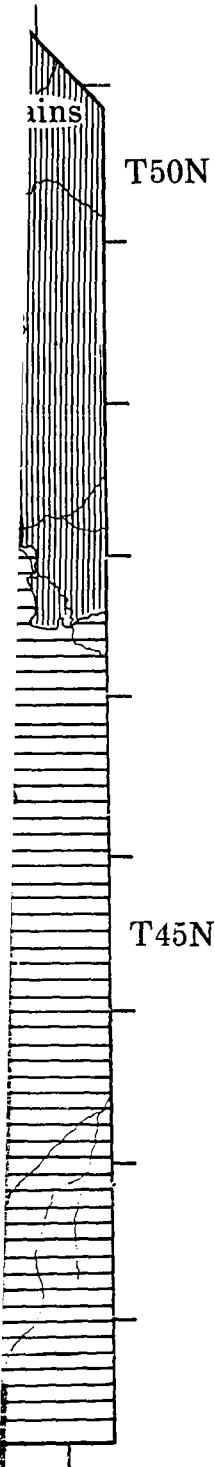
Willwood Formation

Marginal conglomerate & lenticular sandstone grading basinward to channel and sheet sandstones interfingering with variegated mudstones; occasional lignites.



Pre-Cambrian rocks, undivided

Mainly granitic rocks, with lesser amounts of metamorphics.



Mean Orientation of Paleocurrent
Direction Indicators. Number
Refers to Locality Designation

REVIEW OF PREVIOUS WORK

Geologic investigations of the Willwood Formation were initiated in the late nineteenth century by Cope (1882), who presented descriptions of the early Eocene, red-banded strata and their mammalian fossil content. Early workers correlated the Tertiary exposures with the fossiliferous portion of the Wasatch in southwestern Wyoming and northeastern Utah and proposed a lacustrine origin for the strata. Detailed studies led Fisher (1906) and Loomis (1907) to postulate a fluviatile mode of origin for the Big Horn "Wasatch". Sinclair and Granger (1911, 1912) and Granger (1914) confirmed earlier fluviatile hypotheses and subdivided the Lower Eocene "Wasatch" into a series of faunal zones.

Van Houten (1944) pointed out the confused usage of the term Wasatch over the years (Fig. 2) and proposed in its place the Willwood Formation. Additional reports by Van Houten (1945, 1948, and 1961) presented important information concerning the stratigraphy and paleontology of the Willwood and the origin of red-banded strata throughout the Rocky Mountain region. Recent studies of Willwood exposures in the Sheep Mountain and Tatman Mountain area in the central portion of the Basin have been reported by Rohrer and Gazin (1965) and Neasham and Vondra (1967).

Fig. 2 Development of terminology.

Epoch	Age	Cope	Loomis	Osborn	Sinclair and Granger	Granger	Osborn	Wood et al.	Van Houten
		1882	1907	1909	1912	1914	1929	1941	1945
Early Eocene	late	Wasatch	Big Horn Wind River formation	Coryphodon zone	Lost Cabin formation	Lost Cabin beds	"Big Horn E" <i>Lambdolerium</i> zone	Lost Cabin Equiv.	Lost Cabin Faunal Zone
	middle	Wasatch group	"Wasatch" formation		Wind River Lysite formation	Lysite beds	"Big Horn D" <i>Haplodon</i> zone	Lysite Equiv.	Lysite Faunal Zone
	early		formation		Wasatch Knight formation	Gray Bull beds	"Big Horn C" <i>Systemodon</i> zone	Gray Bull member	Gray Bull Faunal Zone
Late Paleocene	Clark-forkian				Big Horn Basin "Wasatch"		"Big Horn Wasatch"		
					Clark Fork beds	Sand Coulee beds	"Big Horn A" <i>Phenacodus</i> zone	Polecat Bench fm.	Clark Fork member
							"Big Horn B" <i>Echippus</i> zone	Big Horn "Wasatch"	Willwood Formation
									Polecat Bench Fm
									Clark Fork Faunal Zone

REGIONAL STRATIGRAPHY

Stratigraphic Relationships and Thickness


The Willwood conformably overlies the Paleocene Polecat Bench Formation (Fort Union equivalent) in the central portion of the Big Horn Basin (sec. 29, T51N, R93W). Westward the lower contact grades into an angular relationship, first with Polecat Bench deposits (sec. 7, T48N, R99W) and finally with Upper Cretaceous strata along the Absaroka Mountain front (sec. 7, T48N, R103W). In areas of Polecat Bench-Willwood conformity the establishment of a suitable formational boundary is difficult. As proposed by Van Houten (1944), the first occurrence of red-banding appears to be the best criterion for distinguishing between the two formations. The Tatman Formation, late early to early middle Eocene, conformably overlies the Willwood (sec. 13, T50N, R97W). The contact is gradational and represented by a transition zone of variegated red and drab mudstones intercalated with thin carbonaceous shales.


The thickness of the Willwood decreases from the topographic center of the Basin to its margins. Estimates of maximum thickness have varied, with 2500 feet (Van Houten, 1944) accepted as a good approximation. A stratigraphic section measured from the conformable Polecat Bench-Willwood contact exposed along Antelope Creek 5 miles southwest of Basin, Wyoming to the Willwood-Tatman contact on the eastern slope of Tatman Mountain (Fig. 3) indicated a formational thickness of


Fig. 3 Graphic sections of the Willwood Formation in central portion of the Big Horn Basin.


GRAPHIC SECTIONS OF THE WILL


EXPLANATION

 Lt. gray (N7)

 Pale reddish brown (10R 5/4)
or
Moderate red (5R 1/6)
or
Grayish purple (5P 4/2)

 Pale olive (10Y 6/2)
or
Grayish green (10G 5/2)


 Brownish black (5YR 2/1)

 Interbedded red and drab colors

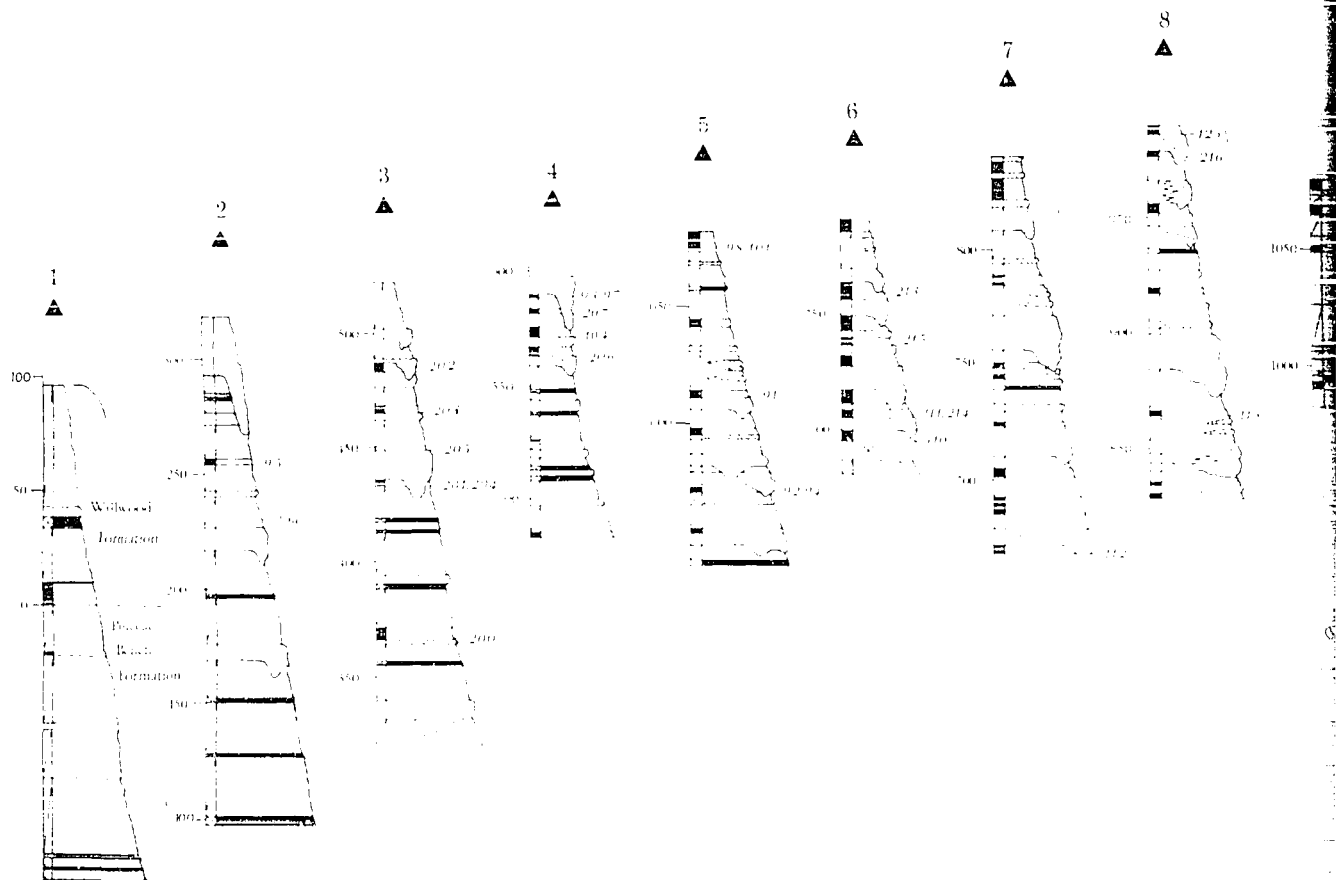
 Sandstone

 Mudstone

 Carbonaceous shale

 4
Location of outcrop section

 Correlation line



NS OF THE WILLWOOD FORMATION

EXPLANATION



Sandstone



Mudstone



Carbonaceous shale

4

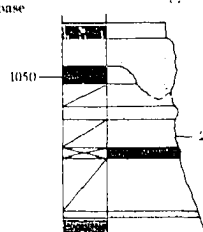


Location of outcrop section

Correlation line

Feet above
base

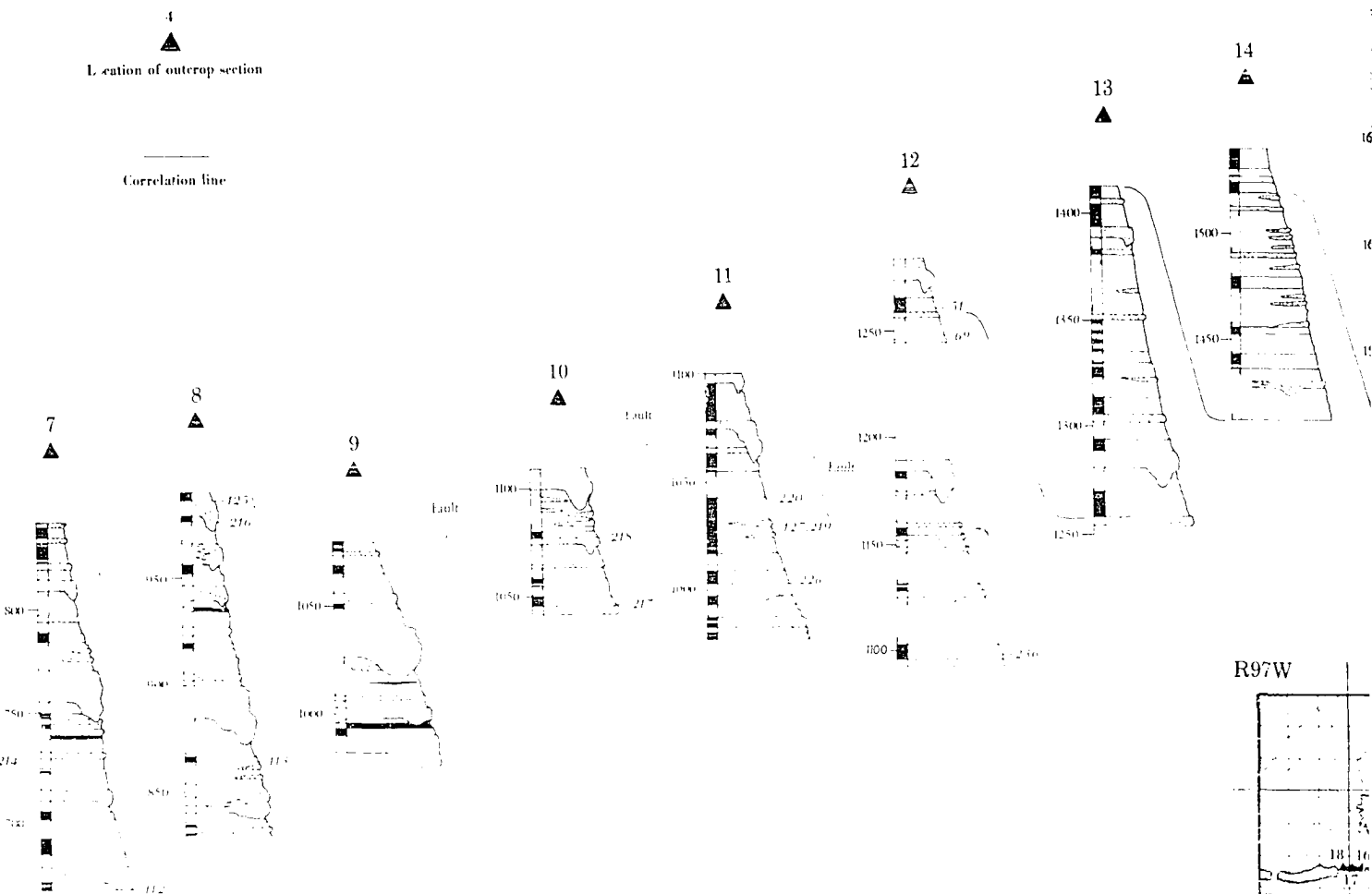
Color Lithology



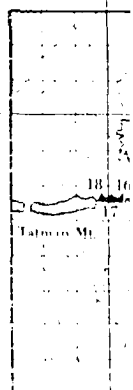
Yale Peabody Museum

fossil locality

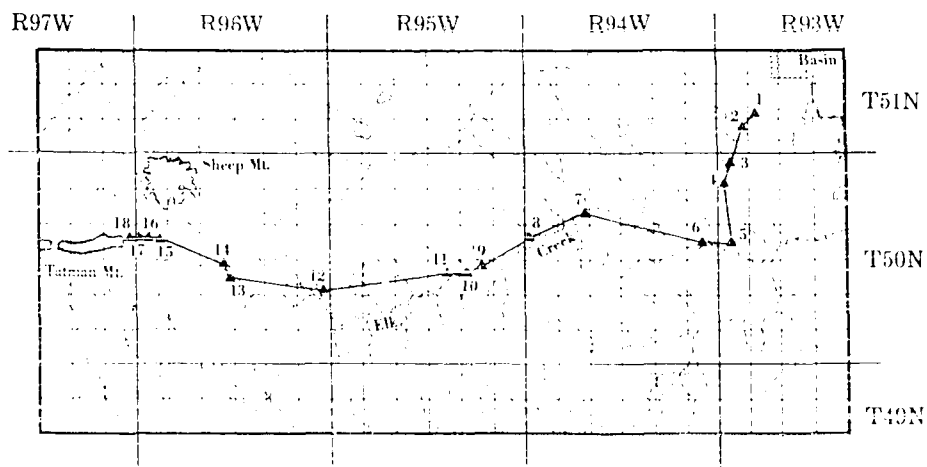
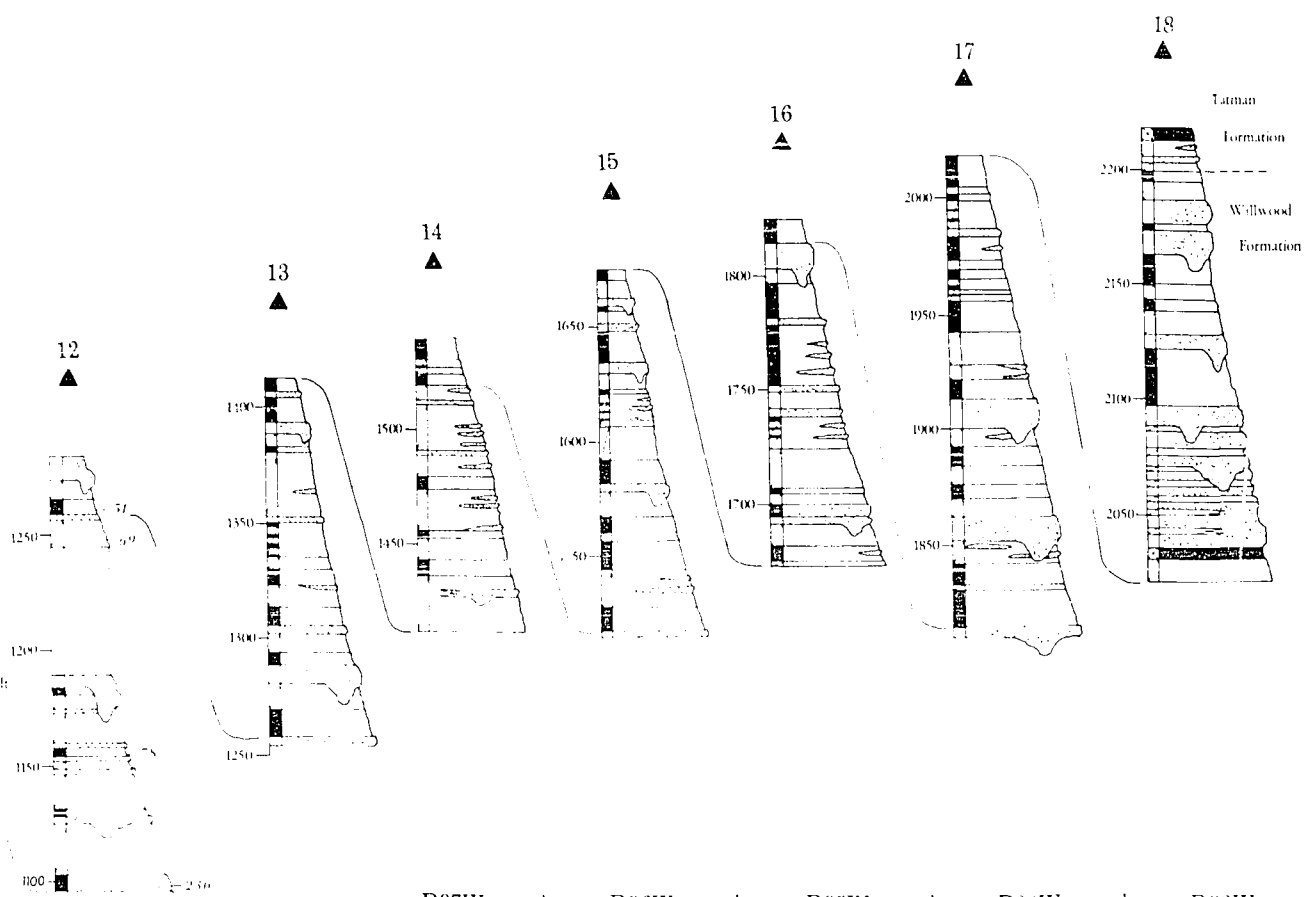
202



R97W



000000



LOCATION OF SECTIONS

approximately 2300 feet. A second section was extended from the angular Polecat Bench-Willwood boundary 12 miles southeast of Meeteetse, Wyoming to the upper Willwood contact on the southern flank of Tatman Mountain. The total thickness measured here was 1320 feet, demonstrating a decrease in thickness to the west of approximately 1000 feet.

Lithologic Facies

The Willwood Formation consists of marginal conglomerates, sandstones, variegated mudstones, and localized carbonaceous shales representing a portion of the Paleogene influx of terrestrial sediments into the Big Horn Basin. Although the formation consists of a varied association of sediments (Fig. 4), two major facies composed of essentially uniform or uniformly alternating lithologies can be recognized.

Conglomerate facies

Marginal Willwood deposits bordering the Absaroka Mountain front include numerous exposures of thick conglomeratic sequences. Interbedded and interfingering pebble and cobble conglomerates and sandstones outcrop in the vicinity of Meeteetse, Wyoming (Fig. 5). Individual beds range from 7 to 10 feet in thickness. Primary sedimentary structures are abundant and include large scale trough and tabular cross-stratification, horizontal bedding, graded bedding, and numerous cut-and-fill relationships. Mudstones are rare to absent. Occasional granule and pebble conglomerates outcrop in the

Fig. 4 Photographs of Willwood lithologic facies.

- a. Sandstone and variegated mudstone facies exposed in the central Basin area (sec. 13, T50N, R96W).
- b. Outlier of Willwood sandstone-mudstone facies cropping out at the foot of the Absaroka Mountains (sec. 7, T48N, R100W).
- c. Interbedded sandstones and conglomerates outcropping near Meeteetse (sec. 19, T49N, R99W).
- d. Cobble-size quartzite conglomerate. Note well rounded nature of particles (sec. 19, T49N, R99W).
- e. Sequence of massive Willwood mixed carbonate and sandstone, cobble and boulder conglomerates exposed along the Beartooth Mountain front (sec. 35, T57N, R103W).
- f. Close-up view of mixed carbonate and sandstone cobble and boulder conglomerates shown in photograph 4e.

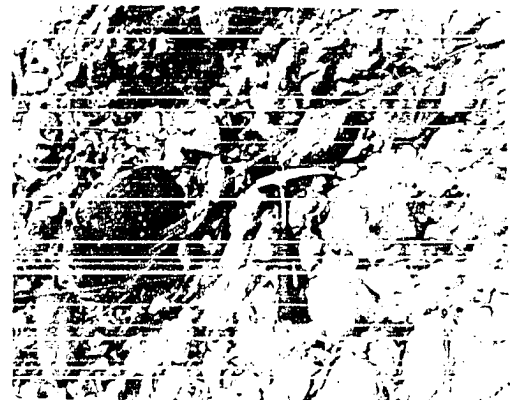
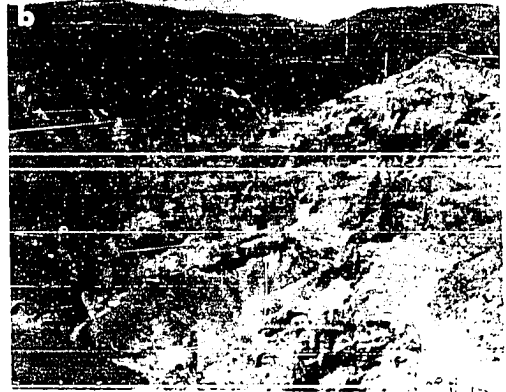
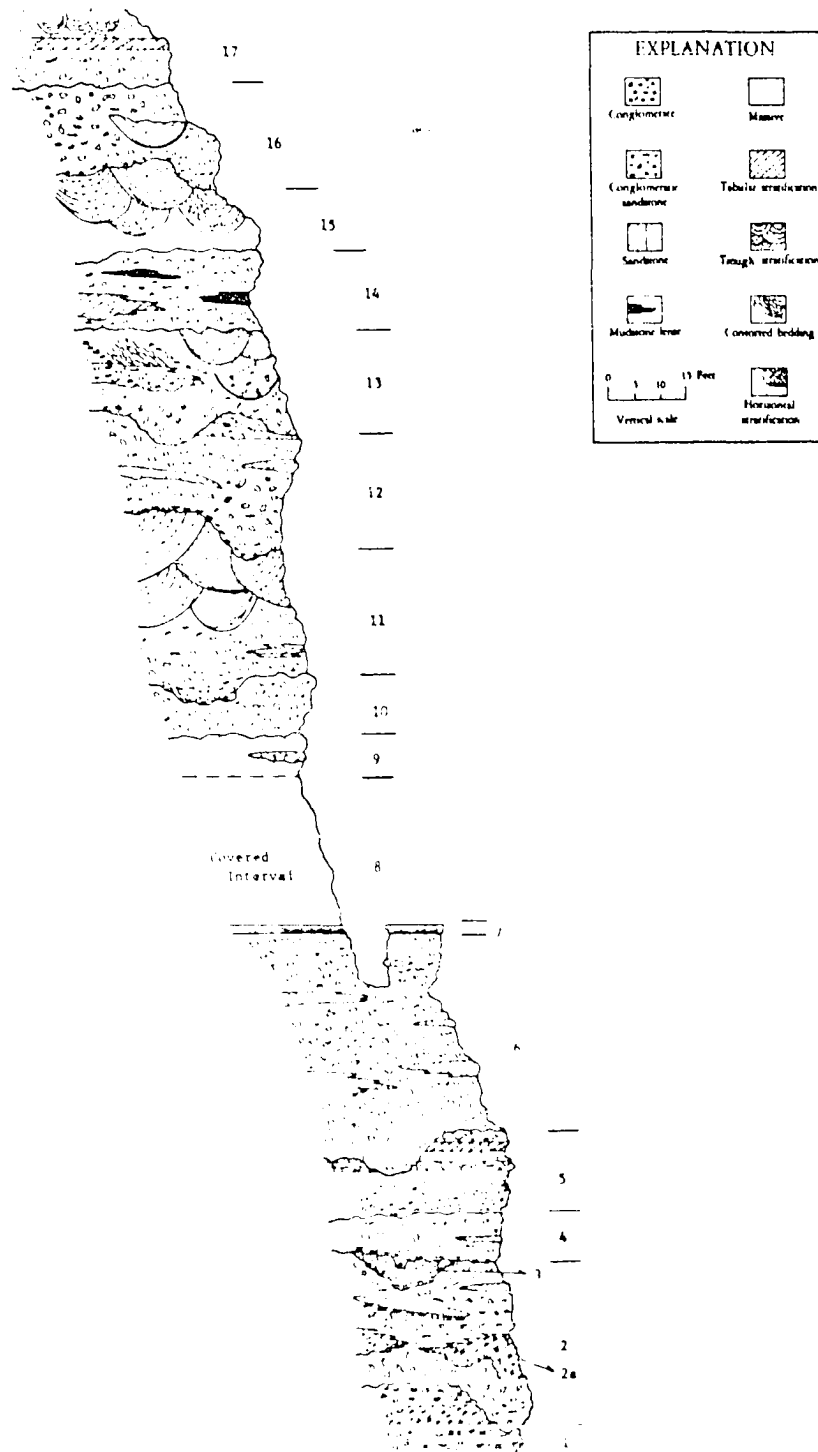


Fig. 5 Graphic section of Willwood conglomerates exposed near the town of Meeteetse.

Five miles northeast of Meeteetse,
Wyoming NW1/4, SE 1/4, Sec. 19,
T49N, R99W



southern (sec. 2, T45N, R95W) and southeastern (sec. 8, T45N, R89W) portion of the Basin. These are similar to those exposed near Meeteetse except that carbonate extraclasts compose a significant component of the detrital material. Extensive exposures of mixed, acid igneous granite and metaquartzite pebble and cobble conglomerates outcrop in a series of prominent hogbacks paralleling the Beartooth Mountain front in the northwestern portion of the Basin (Fig. 6, sec. C-C'). The geometry of the conglomerates varies from thin stringers and localized lenses to tabular units ranging up to 30 feet thick. These are commonly interbedded with sandstones and occasionally with mudstones higher in the section. Mixed carbonate and sandstone, cobble and boulder detrital material also constitute prominent conglomerates in the Beartooth Mountain front area (Fig. 6, sec. A-A'). Steeply dipping beds of the lower 650 feet of the exposure display a limestone cobble conglomerate interrupted by only a few, thin, tabular sandstone beds.

Sandstone and mudstone facies

The Willwood Formation consists predominantly of lenticular and sheet sandstones, variegated tabular mudstones, and a few thin lenticular carbonaceous shales in the central portion of the Basin. When viewed from a distance, color banding gives the strata a simple, laterally and vertically homogeneous appearance. Close examination, however, reveals a more intricate nature. Rock units may grade laterally and

Fig. 6 Graphic sections of the Willwood along the Beartooth Mountain front.

WILLWOOD SECTIONS ALONG

Interbedded sandstones and
red mudstones

SECTION D - D'

Granite & quartzite
pebble conglomerate

SECTION C - C'

Quartzite
pebble conglomerate

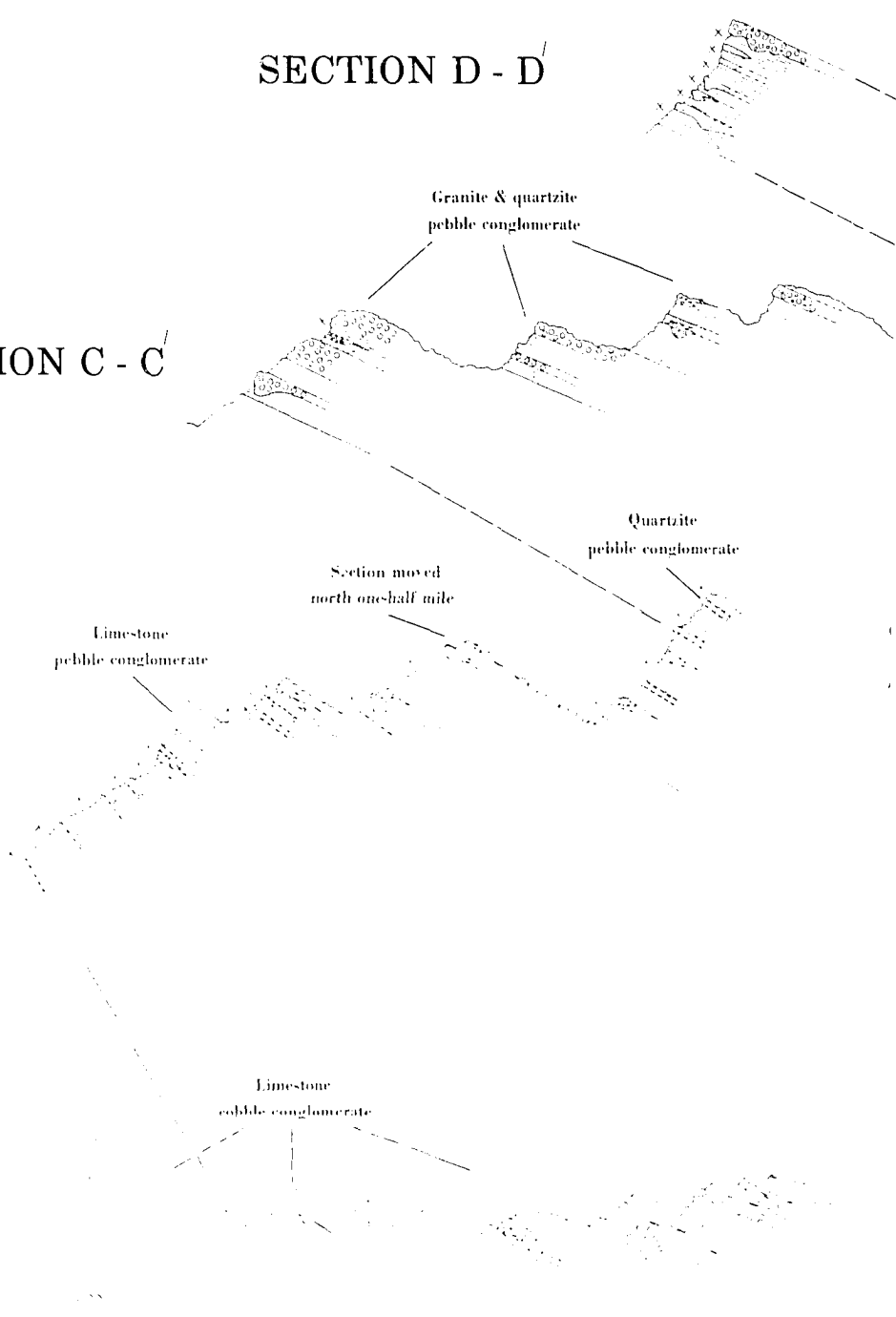
Section moved
north one-half mile

Lime-stone
pebble conglomerate

SECTION B - B'

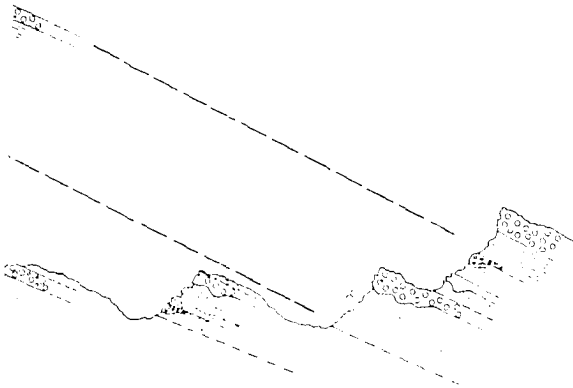
Lime-stone
cobble conglomerate

SECTION A - A'



LONG BEARTOOTH MOUNTAIN FRONT

s and



R10

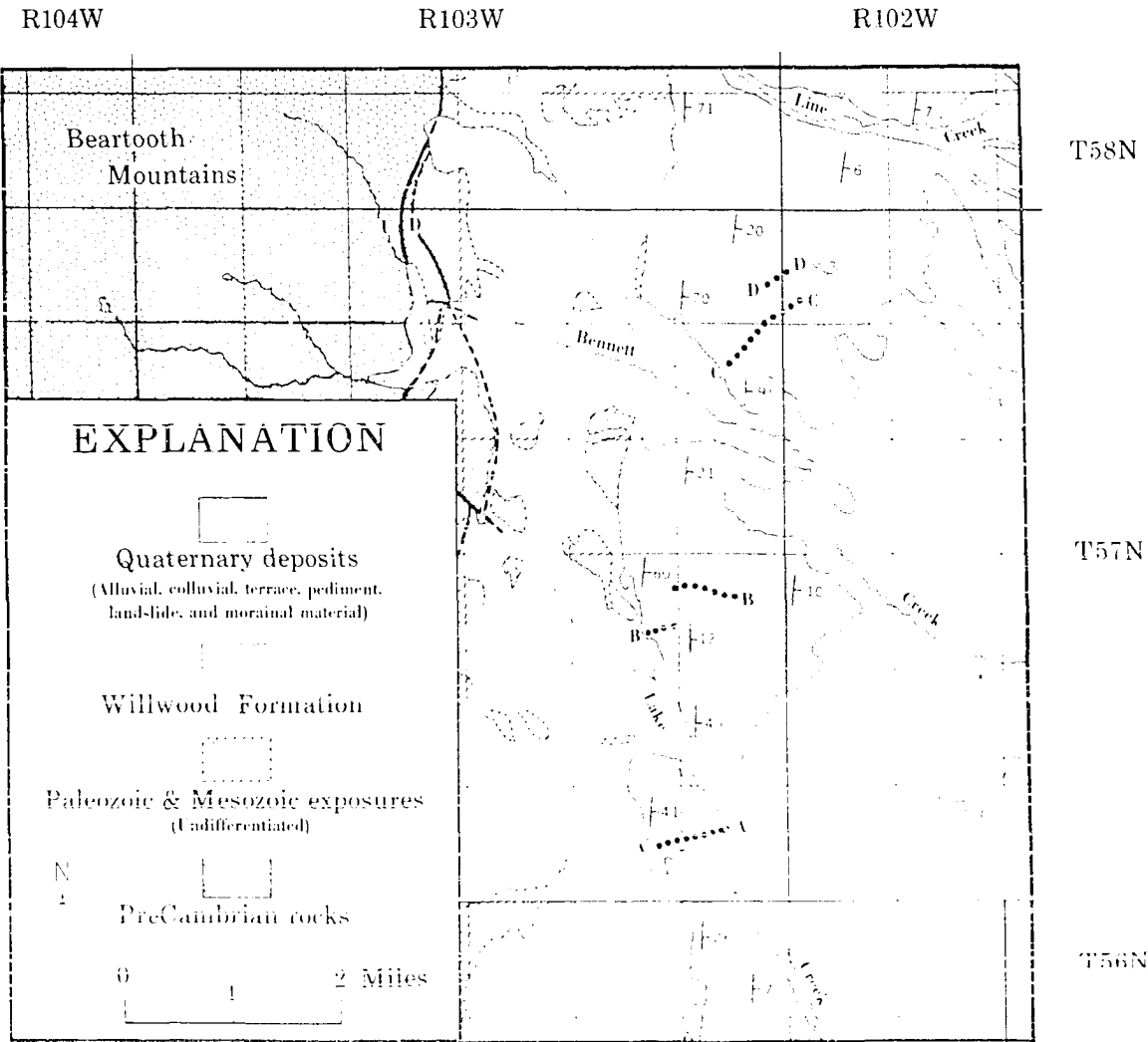
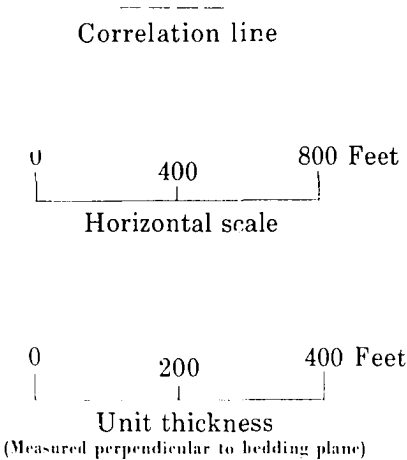
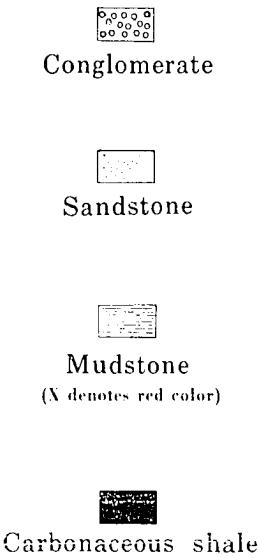
Cover

Granite
pebble conglomerate

Granite
pebble conglomerate



EXPLANATION



Geology after Pierce (1965)

LOCATION OF SECTIONS

vertically into one another, wedge-in and pinch-out over variable lateral distances, or truncate adjacent units.

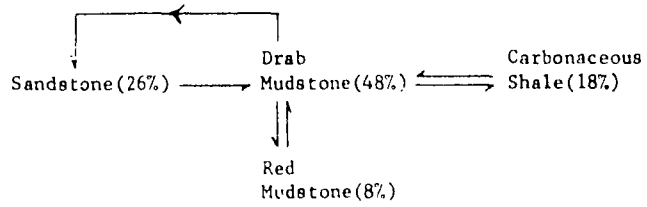
Initial examination of the sediments suggests an unordered bedding sequence. Division of the Basin-Tatman Mountain traverse into a lower, middle, and upper portion and the application of a statistical Markov chain analysis (Gingerich, 1969), however, demonstrates the presence of repetitive depositional sequences. Derived vertical lithic transitions, with relative percentages of rock types for each portion of the Willwood, are presented in Fig. 7. A complete sequence is not common, with incomplete cycles often marked by the absence of one or more medial units or the premature occurrence of the basal sandstone unit of an overlying sequence.

The repetitive depositional sequence begins with a basal lenticular sandstone and associated thin, lateral sheet sandstones. The lenticular sandstone, generally light gray (N7) to yellow gray (5Y7/2) occupies a linear depression eroded into older strata. Thin sheet sandstones extend laterally from its upper portion. In the lower portion of the Willwood the basal lenticular sandstone grades vertically into drab pale olive (10Y6/2) and grayish green (10GY5/2) mudstones. Overlying units commonly include either thin lenticular carbonaceous shales or, to a lesser extent, red (10R5/2) mudstones. The uppermost unit of the sequence is another drab mudstone, which is overlain by a basal lenticular sandstone marking the initiation of a new depositional sequence. The cycles of the

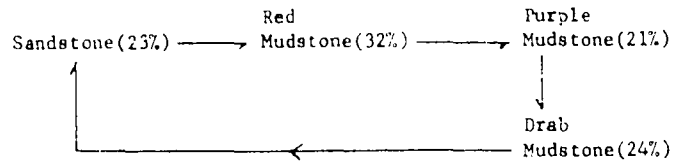
Fig. 7 Vertical lithic transitions of sandstone-mudstone facies derived from Markov chain analysis.

BASIN - TATMAN MOUNTAIN SECTION

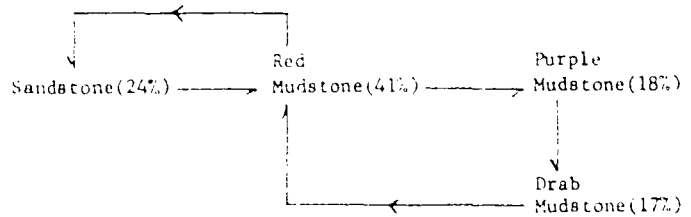
Lower Portion (700')
 93 beds
 $\bar{X}_b = 19.4$
 $P = .015$



Middle Portion (1000')
 208 beds
 $\bar{X}_b = 52.4$
 $P < .001$

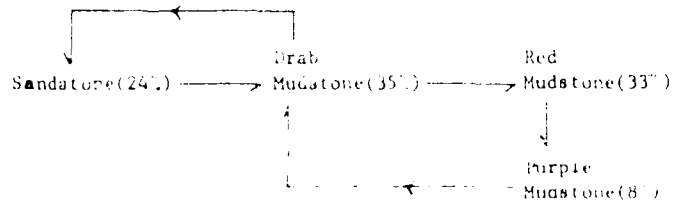


Upper Portion (600')
 95 beds
 $\bar{X}_b = 36.5$
 $P < .001$



MEETEETSE - TATMAN MOUNTAIN SECTION

Entire Section (1300')
 217 beds
 $\bar{X}_b = 16.05$
 $\bar{r} = .64$



middle and upper portions, while showing several similarities to each other, differ from the lower Willwood sequence. They both display thin basal lenticular sandstones which grade vertically to a red (5R4/6) mudstone, purple (5P4/2) mudstone, and olive gray (5GY5/2) mudstone sequence. They differ, however, in that the olive gray mudstone terminates the sequence of the middle portion of the Willwood, while the top most bed of the upper portion is another red mudstone.

Mudstone units are uniformly dominant, comprising approximately 75% of the Willwood. Drab mudstones dominate the lower portion of the Willwood, with red mudstones becoming increasingly more abundant higher in the Formation. Carbonaceous shales are significant only in the lower portion. Ninety percent of the purple mudstones described along the Basin-Tatman Mountain traverse occur as thin beds capping red mudstones. Many purple units may be traced laterally for several miles.

A Markov chain analysis of the Willwood measured along the Meeteetse to Tatman Mountain traverse yields a similar vertical lithic sequence (Fig. 7). The dominance of drab mudstones, a red to purple mudstone sequence, and a 1:4 sandstone-mudstone ratio are similar to the Basin-Tatman Mountain traverse. No carbonaceous shales were recorded. Although the chi-square test gives a higher P value (.04) than that for the other sequences, it can still be considered as statistically significant (Folk, 1968).

PETROLOGY

Investigations of the textural and mineralogical aspects of the Willwood Formation necessitate a variety of qualitative and quantitative analytical techniques. The standard petrologic methods of thin-section examination, feldspar staining, heavy mineral separation and identification, and X-ray diffraction were employed in an analysis of the main rock-forming minerals. In addition, pipette, titration and atomic absorption analyses were utilized for more detailed examination of mudstone texture and composition. A few sandstones from the Polecat Bench (PB) and Tatman (T) Formations are included for comparison purposes.

Conglomerates

Genetically, the Willwood Formation contains two types of conglomerates. Extraformational types, volumetrically the most important, are composed of detrital material originating outside the basin of deposition. Three general compositional assemblages may be differentiated.

(1) Metaquartzite conglomerates, which are best exemplified by outcrops east and southeast of Meeteetse (Fig. 5) and west of Winchester in sec. 2, T45N, R95W. Texturally, the coarser material is of a moderately-well sorted, pebble-size nature, with occasional lenses of poorly sorted, granule, pebble, cobble, and isolated boulder-size (225 mm. dia.)

material also present. Disk, roller, and spherical particle shapes are common, most of an extremely well rounded nature. Percussion marked, metaquartzite particles in a variety of colors comprise the dominant rock-type, with carbonate, sandstone, chert, and igneous rocks present in varying, minor amounts. Matrix material consists of a poorly-sorted, coarse- to fine-grained, argillaceous sandstone, with quartz the dominant detrital mineral. Variations in matrix material tend toward a well-sorted, medium grained, sandstone. Most of the conglomerates described are well indurated, with carbonate, silica, and iron oxide serving as cementing agents within the sandstone matrix.

(2) Conglomerates consisting predominately of igneous rock fragments. These units outcrop in the northwest portion of the Big Horn Basin along the Beartooth Mountain front (sec. C-C' of Fig. 6) west of the town of Clark. Well rounded pebble- and cobble-size igneous rocks, comprising approximately two-thirds of the total mineralogy, include predominately acid igneous varieties. Intermediate igneous and metamorphic rocks, coupled with occasional carbonates and sandstones, are present in minor proportions. The conglomeratic material is generally set in a coarse- to medium-grained sand matrix.

(3) Willwood conglomerates of carbonate and sandstone detrital material are exposed in the same general area as (2). Section A-A' of Fig. 6 illustrates a thousand foot section measured through these units. The conglomerate beds, up to

260 feet thick, consists predominately of carbonate "extra-clasts" (Wolf, 1965). Sandstone cobbles comprise a significant minority, while cobbles of chert, silicified fossil algae (Mississippian age), intraformational conglomerate (Cambrian age), granite, and quartzite are rare. Particle diameter varies from cobble to boulder-size in the lower portion to pebble-size higher in the section. Conglomeratic material is generally well rounded and set in a sand matrix and carbonate cement.

Intraformational conglomerates constitute the second type. These conglomerates are uncommon and occur only in the basal, axial portion of lenticular sandstones. The fragments are composed of mudstone and carbonate concretions apparently derived from slumping of semi-consolidated bank material into an active stream channel.

Occasional conglomerates display characteristics intermediate between intraformational and extraformational types. Numerous rounded clay clasts, up to 8 mm. in diameter and of a grayish yellow green (5GY7/2) color, are contained in the basal portion of extraformational conglomerate and coarse sandstone units. Often such clasts occur as thin stringers extending for several feet along sandstone beds. Drifted logs up to 1 foot in diameter were recorded in a few Willwood sandstones.

Sandstones

Mineral composition

Percentages of grains, cement, matrix, and composition were determined (Fig. 8) from 300 point counts per thin section of 18 sandstones taken along the Basin-Tatman Mountain traverse and 8 sandstones from Willwood exposures along the Basin margin, Polecat Bench (PB), and Tatman (T) beds. Framework grains average 73 percent, with intergranular cement and matrix material averaging 27 percent. Most of the sandstones are classified (McBride, 1963) as subarkose, with variations extending into quartzarenite and more "arkosic" categories (Fig. 9).

The dominant mineral in all Willwood sandstones is common quartz, which constitutes an average of 68 percent of the grains in the central Basin Willwood deposits. Distinction between non-undulatory and undulatory varieties was not made because of their gradational nature and the influence of crystallographic orientation (Blatt and Christie, 1963). Very few grains exceeded a 30 degree extinction angle, suggested by Andresson (1961) as useful in distinguishing between plutonic and metamorphic quartz on a flat petrographic stage. Internal features of common quartz grains include fluid vacuoles, bubble trains, and mineral inclusions of euhedral zircon crystals and rutile needles. Other characteristics include etching by calcite cement, silica overgrowths, and the progressive recrystallization of chalcedony and chert to quartz. Particles

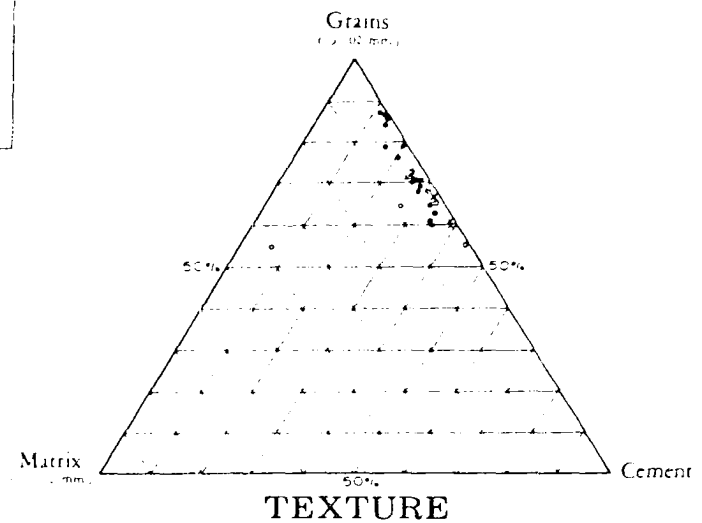
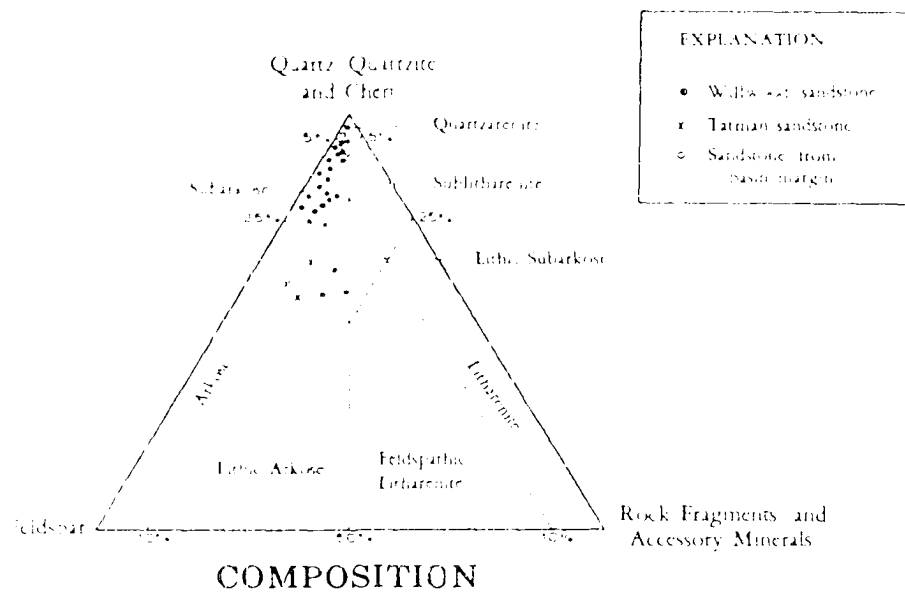
Fig. 8 Percentages of grains, matrix, cement and mineralogical components of Willwood sandstones.

Sample				Composition of Framework Grains				% Misc. Constituents
	% Grains	% Matrix	% Cement	% Common Quartz	% Metaquartzite	% Chert	% Feldspar *	
PB-1	87	0	13	53	11	29	6	1
PB-7	85	1	14	66	7	19	7	1
1-31	60	5	35	74	9	11	11	1
1-35	71	2	27	75	8	8	8	1
1-56	84	2	13	73	8	13	5	1
2-7	70	3	27	70	6	18	6	-
3-17	79	5	16	65	6	11	16	2
5-19	72	5	23	76	7	12	5	-
8-27	64	4	32	51	12	21	14	2
9-1	72	4	24	70	9	10	10	1
12-1	79	1	20	65	6	16	11	2
12-21	68	3	29	64	6	12	16	2
13-35	72	3	25	71	5	19	3	2
15-9	61	5	34	57	7	15	18	3
15-16	62	3	35	71	5	13	7	4
15-39	71	3	26	76	3	6	12	3
16-13	88	-	12	84	4	8	3	1
17-26	77	5	18	59	4	11	22	5
18-37	68	2	30	69	6	10	15	1
5498	69	2	29	62	3	28	5	2
4899 ^o	67	-	33	31	19	7	22	21
4999 ^o	56	-	44	30	15	9	24	22
4797 ^o	65	7	28	41	13	9	20	17
T-2	60	-	40	60	6	9	18	6
T-4	63	1	36	55	3	4	33	5
T-5	66	2	32	47	5	5	31	12

* - Percent feldspar based on both thin-section modal analysis and grain counts of stained disaggregates.

^o - Sandstones from basin margins (4899 represents legal location of sample; T48N, R99W).

Fig. 9 Textural and compositional classification of
sandstones (after McBride, 1963).



range from predominately a subangular variety to a few well rounded and spherical quartz grains (Powers, 1953) indicative of recycled sedimentary detritus. Metaquartz, in the form of polycrystalline grains with intragranular units separated by sutured boundaries and displaying separate, strongly undulose extinction, constitutes an average of 7 percent in the Willwood from the central portion of the Basin. Occasional metaquartz grains show a dominant orientation of elongate intragranular units. Microcrystalline quartz (chert) averages 13 percent of the framework grains.

The feldspar composition of Willwood samples from the central portion of the Basin averages 10 percent. This was analyzed by both petrographic examination and a staining technique developed by Reeder and McAllister (1957) and reported by Vondra (1963). A marked predominance of quartz over feldspar and potash over sodic and calcic feldspar is indicated by both staining and thin section analysis. Orthoclase, similar to quartz in optical color and extinction, has a "fresh", unweathered appearance and may be differentiated by its cleavage and yellowish-orange stain. Microcline, also stained yellow-orange, displays characteristic polysynthetic twinning in the form of grid and subparallel twin lamellae. Perthite intergrowths, unmixing of microcline-albite perthitic components, and occasional sericite alteration were also noted. Extinction angles of albite twin planes indicate plagioclase compositions in the sodic (albite-oligoclase-

andesine) range.

Accessory detrital minerals ("heavy minerals") greater than 2.8 specific gravity, comprising a minor (2 percent) portion of the Willwood sandstones in the central portion of the Basin, include both igneous and metamorphic source terrane varieties. Individual mineral species were identified under the microscope, and the relative abundance of each visually estimated (Fig. 10).

Calcite is the major cementing agent of the Willwood sandstones, with clear, sparry crystals forming an interlocking mosaic within a "disrupted" granular framework. Silica cement in the form of euhedral to subhedral overgrowths in optical continuity with grain nuclei is common. Original grain boundaries are marked by linear traces of dust(?) and corresponding termination of bubble trains.

Comparison of Willwood sandstones of the central portion of the Basin with those of marginal areas of the Basin and with other formations, illustrate a few consistent variations, including: (1) Marginal Willwood samples display a greater proportion of rock fragments, feldspar, and metaquartz (polycrystalline quartz) over common quartz and tend toward a lithic arkose composition. (2) Tatman sandstones show an increase in feldspar at the expense of common quartz and a higher percentage of cement. (3) The relative proportion of opaque and igneous minerals decrease and metamorphics, particularly garnet, increase vertically through the Willwood and into the

Fig. 10 Heavy mineral frequencies.

Sample	Opaques		Igneous			Nonopaques		Metamorphic	
	Magnetite	Limonite	Zircon	Tourmaline	Rutile	Garnet	Staurolite	Kyanite	Epidote
Lower Willwood									
PR-1	A	F	C	U	-	U	R	-	-
PR-7	F	A	C	U	-	U	R	R	-
PR-8	C	F	U	U	-	U	U	-	-
1-22	U	A	C	C	R	C	U	U	-
1-31	A	A	C	U	-	U	R	R	R
1-35	F	A	C	U	R	C	U	-	-
1-56	U	C	C	C	-	C	U	R	-
2-7	A	A	C	C	R	U	U	R	-
3-11	C	F	C	U	-	C	R	R	-
4-11	U	A	C	C	-	C	U	-	-
Middle Willwood									
6-17	A	C	U	U	-	U	R	R	-
8-10	U	U	A	U	R	U	U	U	-
9-1	A	C	A	C	R	U	R	R	-
11-15	U	C	C	C	-	C	U	U	-
Upper Willwood									
13-8	U	A	A	U	-	C	R	R	U
13-28	C	U	C	U	-	A	U	R	-
13-35	U	A	A	U	R	C	U	R	R
15-9	U	C	C	R	R	C	U	R	-
15-16	C	U	U	U	-	C	U	U	R
15-39	C	C	U	R	-	C	U	-	-
16-5	A	A	C	C	-	C	U	-	-
17-26	A	C	C	C	-	U	U	R	-
18-27	C	R	U	R	-	A	U	R	-
18-37	U	C	U	U	-	A	U	-	-
Tatman Formation									
T-1	C	U	R	R	-	F	C	R	R
T-2	A	U	R	R	-	F	C	U	R
T-4	C	R	U	-	-	F	U	R	R
T-5	C	R	U	R	-	F	U	U	R

F - Flood (45%)

A - Abundant (22-45%)

C - Common (10-25%)

U - Uncommon (2-10%)

R - Rare (2%)

Tatman Formation.

Texture

Textural parameters were tabulated from raw distribution data obtained by optically measuring the long axis of 125 grains per thin section. The statistical measures of mean size (M), standard deviation (σ), skewness (S_k), and kurtosis (K_g) were calculated from formulas developed by Folk and Ward (1957). Fig. 11 records textural data for each sample.

Willwood sandstones examined display an average mean size of 2.59 ϕ (.17 mm.; fine sand), with a standard deviation of .39 ϕ units. Thus, approximately two-thirds of Willwood samples analyzed have average grain sizes between 2.19 ϕ and 2.97 ϕ . Tatman sandstones are somewhat coarser, with samples analyzed giving an average mean size of 2.31 ϕ (.20 mm.; fine sand).

The average standard deviation of Willwood samples is .62 ϕ (moderately sorted), with two-thirds of the samples ranging between .52 ϕ and .72 ϕ . Sorting values for Tatman samples average .56 ϕ . Folk and Ward (1957) and others have noted a relationship of sorting and mean size, with a decrease in mean particle size resulting in better sorted samples independent of distance transported. Thus, for a comparison of sorting values to be significant, mean size should be considered (Fig. 12). Although essentially all samples from the lower, middle, and upper portions of the Willwood Formation

Fig. 11 Statistical measure values of sandstones.

11-1111

Sample	Phi Mean ($\bar{\mu}$)	Phi Deviation (σ)	Phi Skewness (S_k)	Phi Kurtosis (K_k)
PR-1	2.43	0.73	+0.181	1.039
PR-6	3.02	0.82	+0.173	0.780
PS-7	2.78	0.72	+0.216	0.988
PR-8	3.30	0.65	-0.040	1.005
1-22	2.39	0.76	+0.316	0.871
1-31	3.20	0.67	-0.041	0.825
1-35	2.84	0.61	+0.143	0.917
1-37	2.42	0.67	+0.246	0.909
1-56	2.55	0.76	+0.231	0.892
2-7	2.47	0.57	+0.122	0.952
3-11	2.62	0.71	+0.124	0.846
3-17	2.21	0.46	+0.272	0.925
4-11	2.43	0.79	-0.086	0.935
4-12	2.42	0.59	+0.320	1.150
5-6	2.48	0.59	+0.301	0.949
5-19	2.26	0.58	+0.167	1.276
6-14	2.17	0.58	+0.185	0.931
6-31	2.45	0.69	+0.220	0.912
8-27	2.42	0.59	+0.149	0.950
9-6	2.46	0.64	+0.270	0.793
11-5	2.96	0.46	-0.009	0.973
12-21	2.43	0.38	-0.054	1.044
13-6	2.69	0.49	+0.129	0.898
13-28	2.28	0.51	+0.138	0.983
13-35	2.74	0.49	+0.024	0.919
14-25	2.7	0.57	+0.127	1.064
15-9	2.34	0.58	+0.098	1.093
15-16	3.61	0.53	-0.016	1.095
16-5	3.00	0.57	-0.233	0.897
17-13	2.67	0.44	+0.096	0.923
18-27	2.83	0.56	+0.032	0.965
18-37	1.85	0.5	+0.137	0.949
4797 ^o	1.86	0.90	+0.108	0.914
4899 ^u	2.17	0.98	-0.261	0.879
4999 ^o	2.05	0.70	-0.120	0.586
57102 ^o	2.88	0.68	+0.130	0.916
52104 ^o	2.72	0.84	-0.088	0.952
T-2	2.38	0.54	+0.130	1.022
T-6	2.26	0.55	-0.007	0.910
T-5	2.28	0.59	+0.070	0.954

o - Sandstones from basin margin (4797 represents legal location of sample, T-2, 2072).

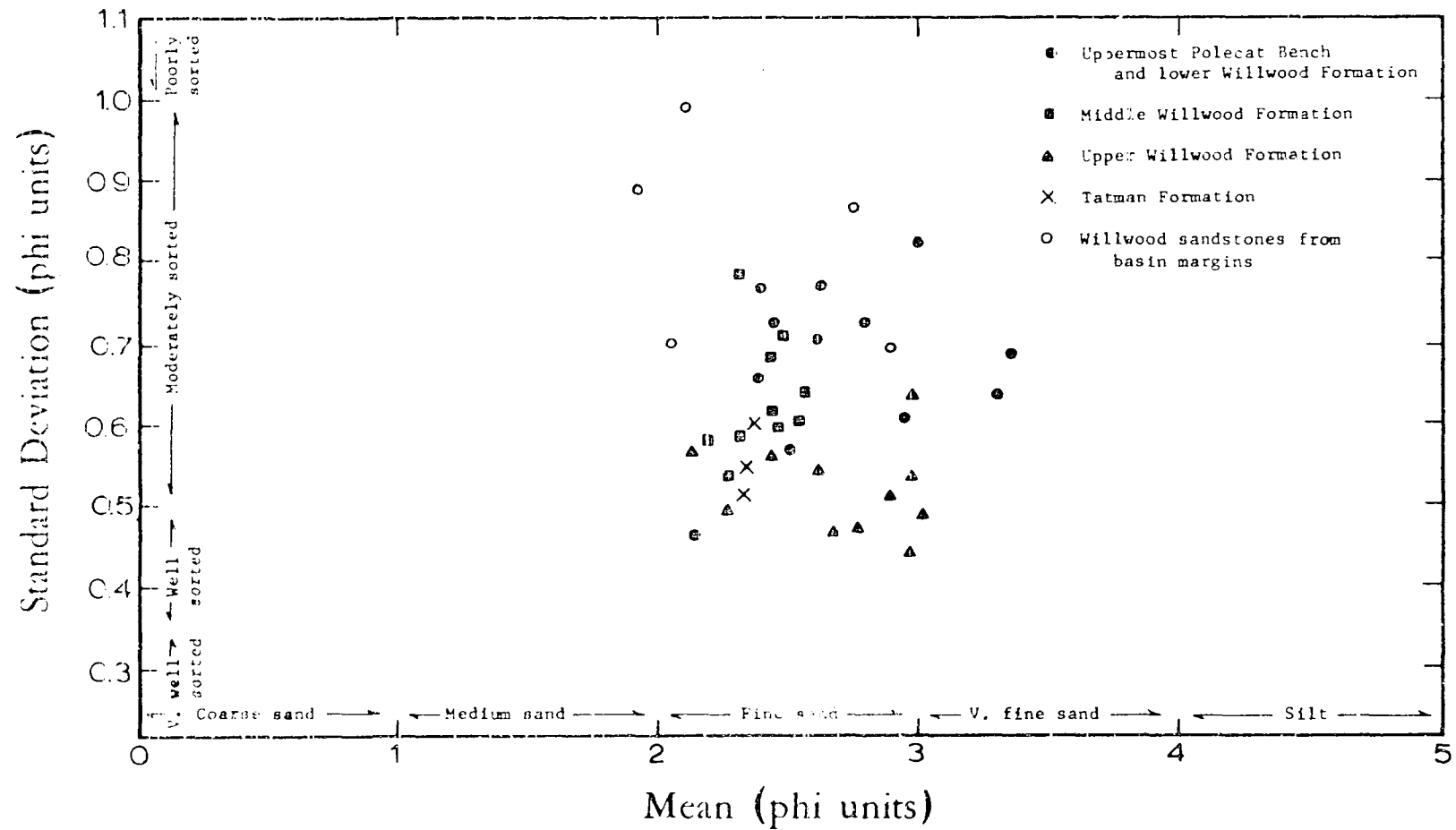
$$\mu_p = \frac{\mu_{1a} + \mu_{1b} + \mu_{1c}}{3}$$

$$\sigma^2 = \frac{\mu_{1a}^2 + \mu_{1b}^2 + \mu_{1c}^2}{3} - \mu_p^2$$

$$S_k = \frac{\mu_{1a}^3 + \mu_{1b}^3 + \mu_{1c}^3}{3} - 3\mu_p\mu_p^2 - 2(\mu_p^3)$$

$$K_k = \frac{\mu_{1a}^4 + \mu_{1b}^4 + \mu_{1c}^4}{3} - 4\mu_p\mu_p^3 - 6\mu_p^2\mu_p^2 - 3\mu_p^4$$

Fig. 12 Standard deviation verses mean size in sandstones.



fall within the 2 ϕ to 3 ϕ range (fine sand), sorting values are .71 ϕ , .60 ϕ , and .54 ϕ , respectively.

Skewness values of Willwood samples, a reflection of the asymmetry of the size distribution, average +0.138 (tail of fines) and have a standard deviation of 0.110. The Tatman sandstones show nearly symmetrical skewness with an average of +0.096.

Kurtosis measures provide a ratio of the sorting of the extremes of the distribution compared with the sorting of the central portion. Average kurtosis is 0.958 (mesokurtic) with a standard deviation of 0.100. Tatman units show similar kurtosis values (0.932).

Skewness and kurtosis measures provide data concerning the "genealogy" of the sediment (Folk and Ward, 1957). Extreme high and low values imply a portion of the sediment achieved its sorting elsewhere in a high energy environment and was transported unmodified to a new environment to be mixed with other sediment. Willwood and Tatman sandstones display normal skewness and kurtosis values, indicating that the grain-size distribution reflects the environment under consideration.

Mudstones

Mineralogy

A qualitative and semiquantitative analysis of the mineralogical composition of 19 Willwood mudstones was performed

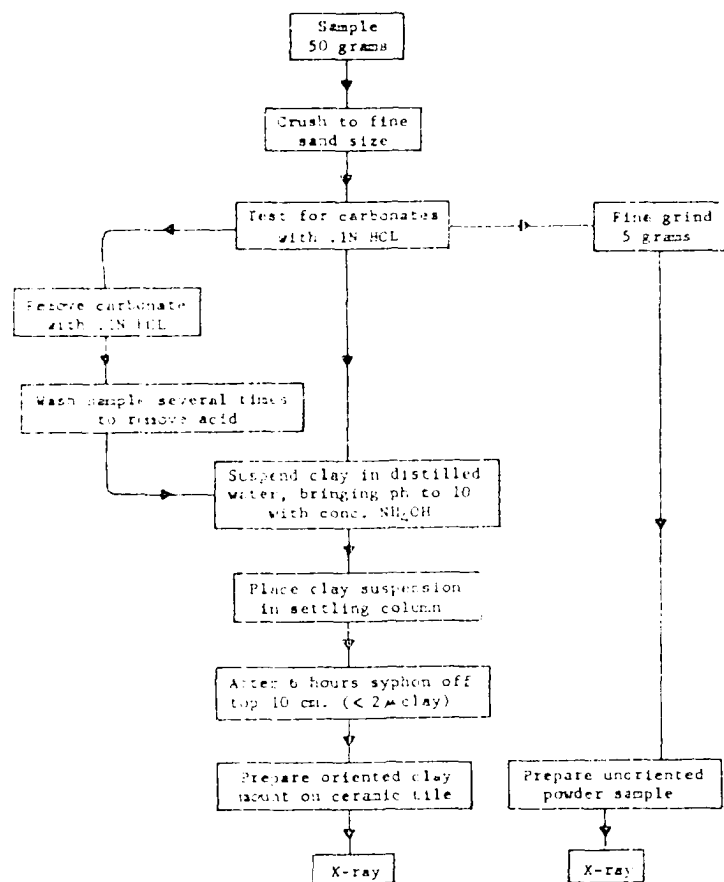
utilizing standard X-ray diffraction techniques (Fig. 13).

Objectives of the determination include: (1) the clay mineral assemblage of red, purple, and drab mudstones and its significance concerning clay mineral genesis in source areas versus in situ clay mineral authigenesis at the site of deposition, and (2) comparisons between mudstones reflecting mineralogical "degrading" during sediment transport. Semiquantitative determination of mineral components follows procedures presented by Schultz (1960) and Shover (1964). Although calculation methods for clay mineral percentages differ, any single method is internally consistent and should give meaningful geologic data (Pierce and Siegel, 1969).

A typical X-ray diffractometer tracing for Willwood mudstones is illustrated in Fig. 14. Quartz and clay minerals are dominant in bulk samples, with feldspar detectable in marginal mudstones. The predominate clay mineral is illite (and clay mica), with contraction and expansion of an asymmetrical "shoulder" on the low angle side of the 10A peak during glycolation and heating suggesting some mixed-layering with a montmorillinite-like lattice. The existence of montmorillinite is indicated by the appearance and disappearance of a 17A peak during treatment. Distinguishing kaolinite and chlorite was difficult and, hence, the weakest part of the semi-quantitative determinations. The 3.53A (004) chlorite peak is "perched" on the high angle side of the kaolinite 3.57A (002) peak, and a comparison of the two gives a rough estimate of the relative

Fig. 13 Flow chart for X-ray analysis of mudstones
(adopted from Raup, 1962).

SAMPLE PREPARATION FOR X-RAY ANALYSIS



X-RAY ANALYSIS TREATMENTS

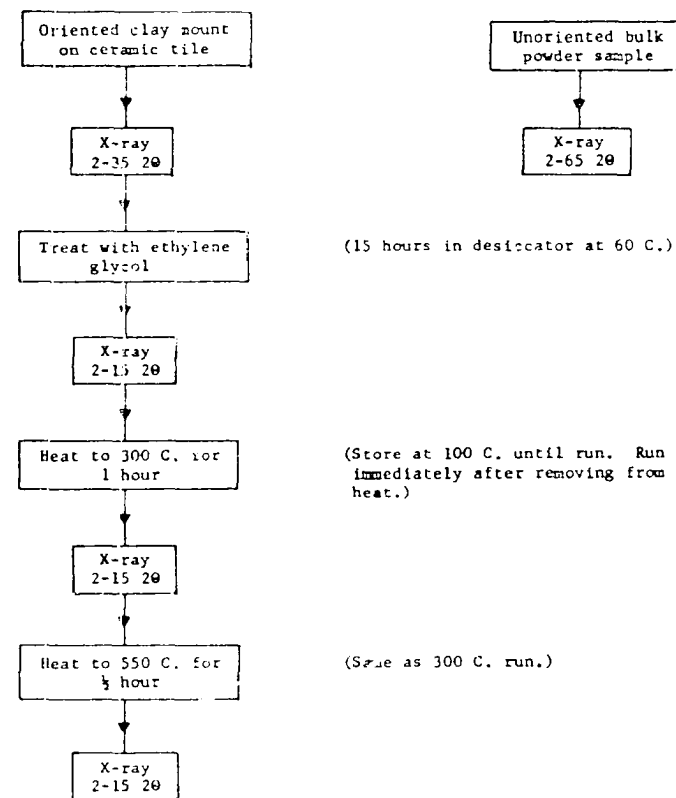


Fig. 14 Typical X-ray diffraction tracing for Willwood mudstones.

amounts of kaolinite and chlorite (Shover, 1964). Diffraction peaks in the 20-30A range were recorded in a few mudstones and probably represent "super-lattice" reflections of mixed-layer clay minerals.

Results of the qualitative and semi-quantitative analyses are presented in Figs. 15 and 16. Inspection of the data yields the following results. (1) No significant differences in mineralogy among red, purple, and drab mudstones is indicated. (2) Illite and clay mica predominates in most samples, averaging 32% of the total clay mineral assemblage. Montmorillonite and kaolinite are present in subordinate amounts, averaging 24% and 18% respectively. Such results basically agree with Willwood clay mineralogy presented by Van Houten (1948). (3) Marginal mudstones differ mineralogically from those of the central Basin area in two general aspects: (a) Mudstones from the Basin margins show a greater feldspar component in bulk sample analyses; and (b) marginal mudstones contain less kaolinite than central Basin mudstones.

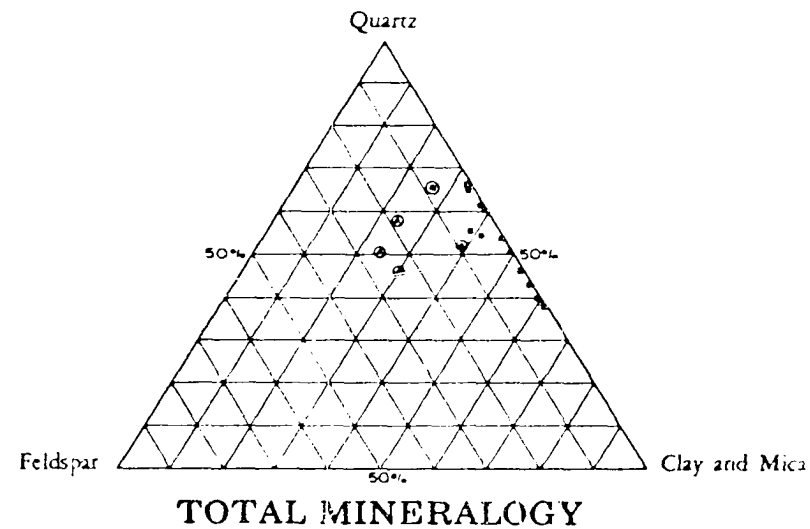
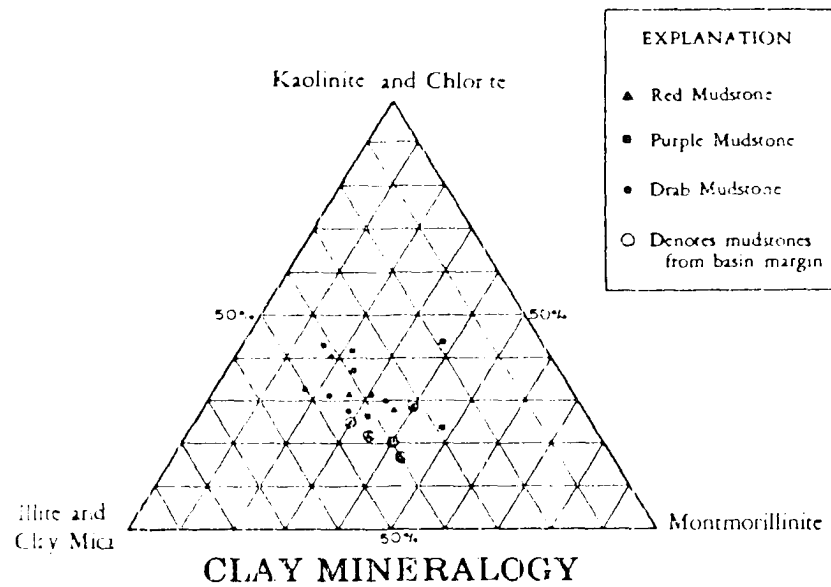
Texture

Particle-size analysis of 10 Willwood mudstones utilizing the pipette method (Folk, 1968) was conducted to gain an approximation of the percentage of clay-size material. Although a high degree of sample consolidation hampered complete disaggregation, an adequate comparison of the amount of material less than 10 ϕ (0.98 μ) on samples analyzed for trace amounts

Fig. 15 Percentages of mineralogical components of
Willwood mudstones.

SAMPLE TYPE AND NUMBER	LEGAL LOCATION	BLOCK SAMPLE				ORIENTED CLAY SAMPLE					
		Quartz	Feldspar	Calcite	Clay & Mica	Kaolinite	Illite	Montmorillonite	Mixed Layer Illite-Mont.	20-30A Clays	Chlorite
Red Mudstone											
10-35R	T50N, R97W	30	tr	25	44	24	47	14	tr	5	9
7'-21	T50N, R96W	52	tr	-	47	27	37	14	10	tr	10
1-1-10	T50N, R96W	55	-	-	45	16	30	35	tr	8	8
43:04R	T48N, R104W	57	18	-	25	11	37	23	5	8	10
52:04R	T52N, R104W	46	24	-	30	7	32	35	8	12	tr
56:00R	T56N, R100W	53	8	tr	39	13	36	29	7	8	6
45:09R	T45N, R89W	50	25	tr	23	17	22	32	13	11	8
53:09R	T53N, R99W	66	tr	tr	53	21	35	21	6	8	7
Purple Mudstone											
6'-29	T50N, R96W	65	tr	-	24	12	22	37	10	10	7
10-35P	T50N, R97W	46	-	-	54	13	32	25	10	12	7
6'-39	T50N, R96W	39	tr	-	60	33	20	30	tr	5	8
48:04P	T48N, R104W	65	7	tr	27	11	32	32	5	13	5
45:05P	T45N, R95W	54	tr	-	44	29	33	10	12	6	9
1-1-27	T50N, R96W	50	tr	tr	48	23	30	18	5	8	11
Dark Mudstone											
4'-22	T50N, R96W	67	-	tr	33	19	34	25	6	9	9
1-1-15	T50N, R96W	43	tr	-	56	16	36	24	8	8	8
1-2-27	T50N, R96W	62	-	-	38	17	36	19	12	9	9
7'-13	T50N, R94W	56	5	5	34	22	33	20	tr	9	12
53:00	T53N, R99W	39	tr	-	60	14	25	25	17	11	8

Fig. 16 Total and clay mineralogy of Willwood mudstones.



of selected chemical constituents (see following section) was obtained.

Chemical constituents

Free iron, aluminium, and manganese plus organic and inorganic carbon were quantitatively measured in 35 Willwood mudstones. Included are red, purple, and drab varieties, and 2 carbonaceous shales. Samples C-12 to C-1, collected at 4 inch intervals from a mudstone sequence outcropping near Meeklem Gulch south of the town of Basin in the upper portion of measured section 4 along the Basin-Tatman Mountain traverse (Fig. 3, fossil locality 207) were also analyzed. Free iron, aluminium, and manganese, extracted from samples by the sodium citrate-sodium hydrosulfite method (Holmgren, 1967), were analyzed with a Perkin-Elmer Model 303 Atomic Absorption Spectrophotometer. Organic carbon percentages were determined using the Walkley-Black titration method (1934) modified by Peech et al (1947). Inorganic carbon in samples was measured on a LECO "70 second carbon analyzer". Objectives of such quantitative analysis were two-fold: (1) to determine and compare the percentages of the selected sediment components among mudstones separated on a color basis; (2) to evaluate in situ mobilization and translocation of such material reflecting soil development.

Examination of the data (Fig. 17) indicates significant chemical variations within the fine grained Willwood sediments analyzed. Organic carbon, preservation of which is generally

Fig. 17 Quantitative data on organic carbon and free iron,
aluminium, and manganese in Willwood mudstones.

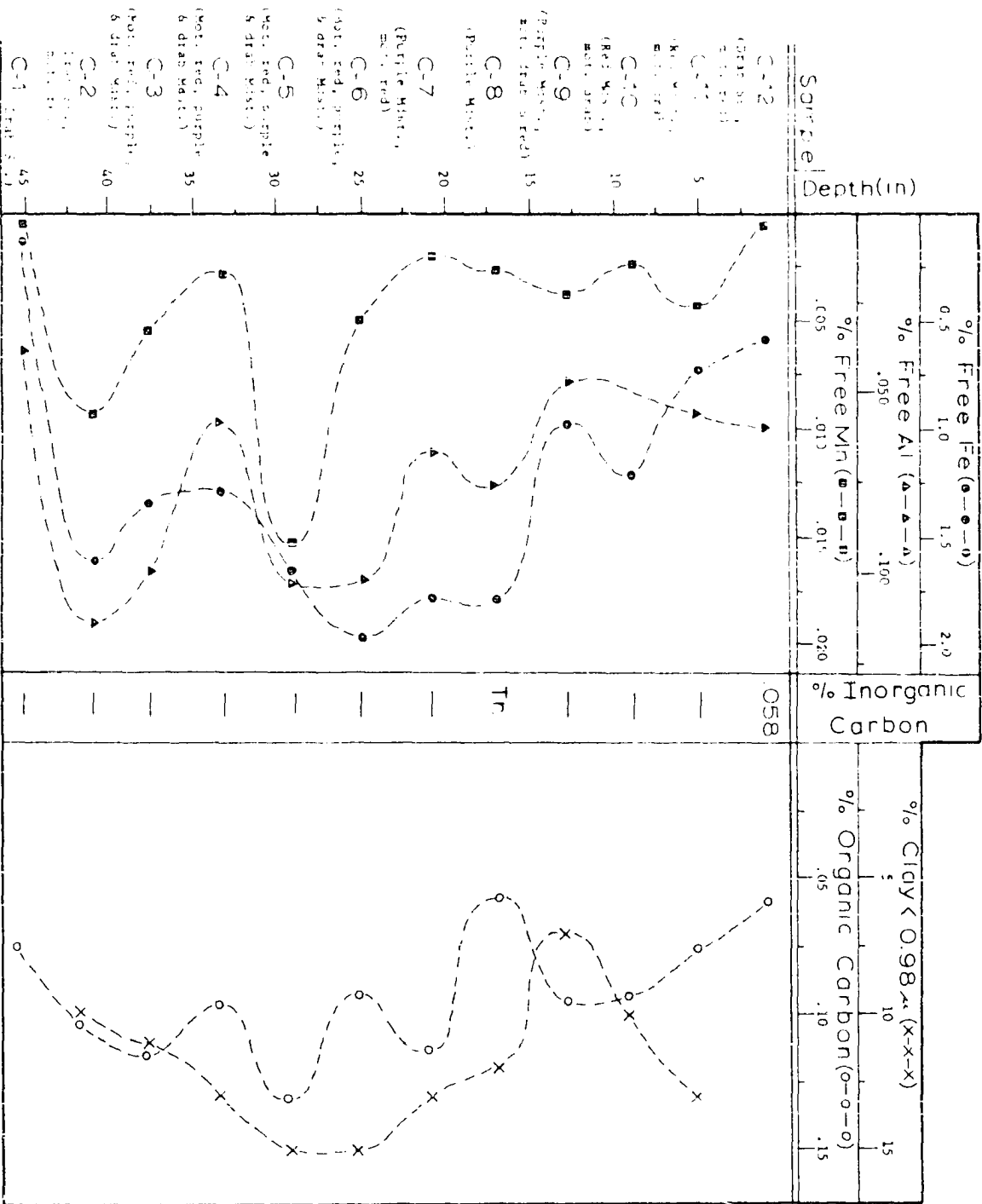
Sample	Wt. % Organic Carbon	Wt. % Free Iron	Wt. % Free Aluminum	Wt. % Free Manganese
Red Mudstones				
4996R	.044	1.67	.106	.0077
52104R	.052	0.96	.049	.0032
56100R	.038	1.67	.114	.0080
48104R	.050	1.79	.095	.0078
16-35R	.038	1.35	.075	.0101
4691R	.010	1.71	.096	.0060
6-12R	.046	1.29	.120	.0096
(Mean)	.040	1.49	.094	.0075
Purple Mudstones				
48104P	.045	1.08	.084	.0078
16-35P	.049	1.48	.067	.0024
4691P	.038	1.76	.097	.0050
6-36P	.023	1.29	.060	.0022
4595P	.034	1.33	.047	.0024
1-1-27P	.052	0.98	.066	.0056
4796P	.047	1.03	.053	.0008
(Mean)	.041	1.28	.068	.0037
Drab Mudstones				
1-22D	.058	1.17	.104	.0009
4791D	.110	0.34	.068	.0010
55103D	.062	0.36	.067	.0014
1-1-15D	.137	0.65	.094	.0034
7-18D	.085	0.61	.069	.0040
6-12D	.081	0.19	.037	.0004
4892D	.046	0.65	.077	.0020
(Mean)	.083	0.57	.074	.0017
Carbonaceous Shale				
L-1	.774	0.24	.270	.0088
L-2	3.372	1.98	.575	.0210
Profile Samples				
C-12	.058	0.59	.059	.0005
C-11	.076	0.73	.055	.0042
C-10	.093	1.23	.067	.0024
C-9	.095	0.98	.053	.0036
C-8	.056	1.79	.074	.0026
C-7	.113	1.78	.065	.0020
C-6	.092	1.98	.101	.0050
C-5	.131	1.06	.101	.0152
C-4	.096	1.30	.058	.0028
C-3	.115	1.35	.099	.0054
C-2	.104	1.61	.113	.0092
C-1	.075	0.13	.036	.0004
(Mean)*	.097	1.44	.079	.0052

* Mean excludes samples C-12 and C-1, which are sandstones.

related to the ground water table and resulting oxidizing verses reducing conditions, is twice as great in drab mudstones as that of red and purple samples. Red and purple mudstones record similar organic carbon values. Inorganic carbon, a reflection of carbonate minerals, was not detected in most of the samples tested. Free iron and manganese progressively decrease in percentage from red through purple through drab mudstones. Aluminium does not show the same relationship to sediment color as iron and manganese, with relatively high values for reds while both purple and drab samples contain similar low values. Carbonaceous shales examined display greater values for all components.

Samples from the mudstone profile C-12 to C-1 show a marked vertical variation in abundance of the chemical components analyzed, with zones of concentration developed at the 16 to 30 inch and 35 to 42 inch levels (Fig. 18). Percent clay less than 10 ϕ diameter also shows a broad zone of concentration in the 16 to 20 inch level. In order to evaluate the possible control of clay content to the other profile components, the sample correlation coefficient r was tabulated (Snedecor, 1956) for the entire profile. Only free aluminium distribution showed a strong direct relationship to clay ($r = +.748$), whereas free iron ($r = +.094$), free manganese ($r = +.160$), and organic carbon ($r = +.004$) display essentially no relationship to clay distribution. As clay minerals are essentially aluminium silicates, a free (extractable) aluminium-clay interdependence

Fig. 18 Vertical distribution of free iron, aluminium, manganese, clay (< 10 Ø), inorganic, and organic carbon from a mudstone sequence.



is not unexpected. Profile variations in the other chemical components, however, appears to be at least partially influenced by factors other than clay content. Unusually high values of organic carbon in the profile as compared with the randomly selected mudstone samples corresponds to the abundance of color mottling. Mottling appears related to bioturbation resulting from increased organic activity (Van Houten, 1948). Unit C-8 lacks mottling and shows a corresponding low value for organic carbon.

SEDIMENTARY STRUCTURES

Fluvial systems generate within their deposits a variety of sedimentary structures reflecting the various processes operating at the site of deposition. Examination of such structures can provide valuable information concerning both the various hydrodynamic factors and sediment supply factors relating to rock genesis, paleocurrents, and paleogeography.

The various sedimentary structures of the Willwood strata are grouped into three major types (after Allen and Friend, 1968): (1) simple structures - those involving one basic lithology and morphology, (2) composite structures - those generally involving more than one kind of lithology and sedimentary structure, and (3) organic structures.

Simple Structures

Sedimentary structures are the product of numerous complex and variable factors of an alluvial channel. Recent investigations of modern sedimentary environments (Allen, 1963a; McKee, 1964; and Middleton, 1965) have supplied important data concerning the qualitative and quantitative nature of sedimentary structures. Of particular significance has been the establishment of relationships between geometric forms (bed configuration) and flow regimes. Although many interrelated variables may influence bed form, stream power (flow regime) and median bed diameter exert a major control in bed form

development (Simons et al., 1965).

Three major stratification types commonly occur in Willwood sandstones. Nomenclature and terminology utilized for their description are drawn from Harms and Fahnestock (1965), McKee and Wier (1953), and Allen (1963a).

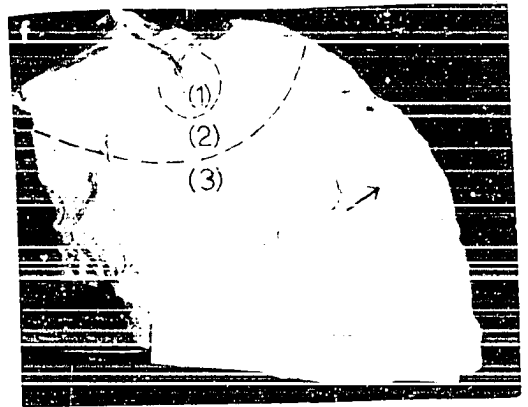
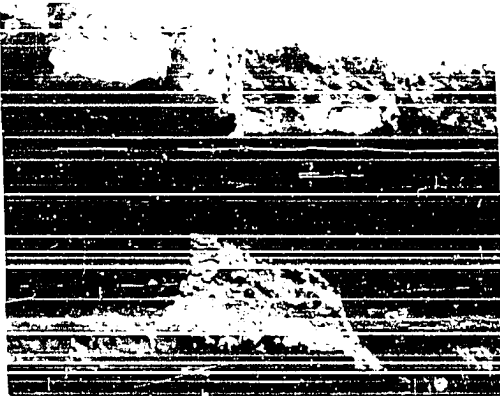
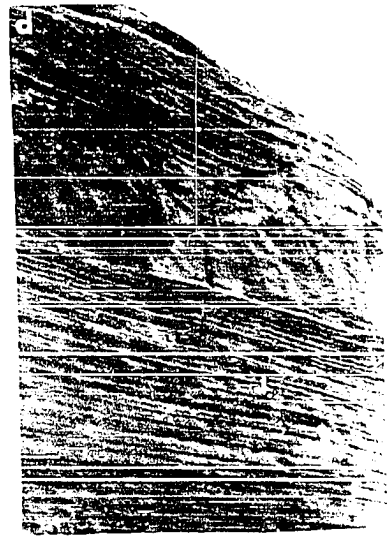
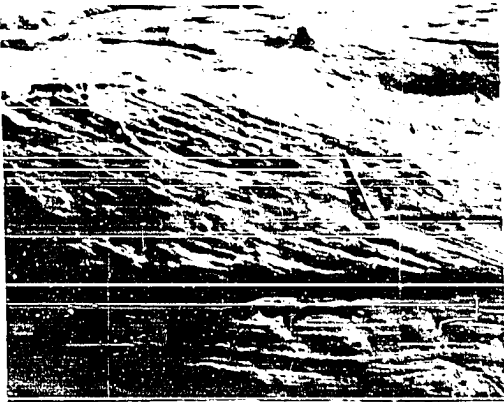
Large-scale cross-stratification

This type includes a sedimentation unit (set) greater than 2 inches thick consisting of laminae (foreset bedding) inclined relative to the horizontal. Cosets of two or more cross-stratified sedimentation units, separated by surfaces of erosion, non-deposition, or abrupt change in character (Allen, 1963a), are the general case in Willwood sandstones. Large-scale trough cross-bedding (pi-cross-stratification of Allen, 1963a) consist of elongate scour channels infilled with curved foreset bedding (Fig. 19a). The scoop-shaped laminae comprise a coset and are either symmetrical or asymmetrical normal to the scour-channel axis. Thin laminae of organic material and basal zones of coarser detrital particles occur in the fills of a few troughs. Allen (1963a) explains large scale trough cross-stratification as resulting from the migration of large-scale, asymmetrical dunes with curved crests, whereas Harms and Fahnestock (1965) postulate the filling of elongate depressions by irregularly shaped migrating dunes in the upper part of the lower-flow regime.

Large-scale tabular cross-stratification (omikron class

Fig. 19 Photographs of simple and organic structures.

- a. Large-scale trough cross-stratification (3) cut into underlying horizontal stratification (2). Large scale tabular cross-stratification are developed at the base (1).
- b. Large-scale tabular cross-stratification developed in pebble-size conglomerates. Individual laminae display graded bedding.
- c. Cosets of small-scale tabular cross-stratification overlying horizontal stratification.
- d. Horizontal stratification interrupted by contorted bedding.
- e. Sand-filled burrows extending downward from sheet sandstone into underlying red mudstone.
- f. Mudstone displaying evidence of organic activity. Arrow indicates worm burrow filled with thin, arcuate laminae. Dark linear trace in upper left portion of photograph is carbonaceous material (plant root?). Zone (1) is grayish yellow green (5GY7/2) sandstone; zone (2) is pale purple (5P6/2); zone (3) is mottled pale purple (5P6/2), dark yellowish orange (10YR6/6), and moderate reddish brown (10R4/6) mudstone.



of Allen) is represented by tabular-shaped, cross-laminated, single and coset units bounded by relatively planar surfaces (Fig. 19b). They are differentiated from trough cross-stratification in that the basal erosional surface exerts little if any control on the configuration of laminae (foresets). Although the individual laminae are generally straight, rare instances of laminae tangential to the lower bounding surface occur. Maximum inclinations average 20 degrees. Allen (1963a) relates omikron-cross-stratification to migrating trains of large-scale asymmetrical ripples with essentially straight crests. Harms and Fahnestock (1965) propose such stratification forms from bars with sinuous, relatively long, avalanche slopes and generally flat upstream surfaces that commonly develop on the downstream margin of point bar deposits during the meandering of a thalweg. They observed that flow regime downstream of the avalanche face, where the loci of tabular cross laminae deposition occurs, is in the lower part of the low-flow regime.

Small-scale cross-stratification

Small scale cross-stratification in the Willwood Formation includes cross-bedded sedimentation units less than 2 inches in thickness. Tabular sets (mu-cross-stratification) are bounded by essentially planar, parallel surfaces, with the cross-laminae generally discordant with the lower bounding surface (Fig. 19c). Allen (1963b) states that such structures could arise from

migrating trains of small-scale asymmetrical ripples with essentially straight crests. Such structures are generally associated with environments involving large and rapid sand accumulation (McKee, 1965).

Horizontal stratification

Horizontal stratification in Willwood sandstones consists of tabular sets of horizontal laminae (Fig. 19d). Individual laminae seldom exceed 1 inch in thickness. The lower bounding surface is generally of a planar, erosional type, whereas upper boundaries may be planar or have superimposed trough cross-stratification erosion surfaces (Fig. 19a). Horizontal stratification is a product of plane-bed or low standing wave transport (Harms and Fahnestock, 1965) marking the lower portion of the upper-flow regime. Such an environment would be expected in restricted alluvial channels during high discharge or on point bar surfaces as accumulating sand creates shoaling conditions.

Composite Structures

Composite sedimentary structures include both channel-fill and overbank deposits representing the lateral and vertical accretion of alluvial detritus within the loof of Willwood deposition. Four major genetic associations occur.

Alluvial fan deposits

Conglomerates and sandstones exposed along the west flank of the Basin display characteristics similar to modern alluvial

fan deposits. Blissenbach (1954), in a discussion of fans of the Santa Catalina Mountains in southern Arizona, noted the rapid cutting and filling of distributary channels by intermittent streams transporting coarse detrital material. Conglomerate exposures in the Meeteetse area (Fig. 5) contain a complex association of scour channels filled predominately with cobble- and pebble-size detritus, with floodbasin mudstones almost completely lacking. Lag gravels (pebble pavement) are developed along basal erosion surfaces, while marginal channel bar deposits of braided streams are recorded by inclined sand lenses containing thin pebble stringers. Rapid pulsatory deposition is indicated by graded-bedding sequences in cross-stratified conglomeratic sandstones (Fig. 19b).

Conglomerates bordering the Beartooth Mountain front (Fig. 6) reflect alluvial fan development on a more localized scale. The lower 650 feet of massive, carbonate and sandstone, boulder conglomerate in section A-A' of Fig. 6 indicate conditions of rapid erosion of a proximal, extra-basinal limestone terrane and a short distance of transport. Thin, interbedded sheet sandstones reflect sheetflood deposits resulting from a stream overtopping its channel and extending laterally over the alluvial fan surface. Vertically, laterally along strike, and down-dip into the Basin the carbonate extra-clast interval grades into interbedded conglomerates, stream channel sandstones, and floodbasin mudstones. Conglomerate petrology changes to igneous and metamorphic detritus at

higher stratigraphic levels, reflecting the stripping of the sedimentary cover and exposure of a Precambrian terrane in the source area. Red mudstones of section B-B' of Fig. 6, laterally equivalent to conglomerates, are interpreted as overbank deposits marginal to the fan proper.

Channel deposits

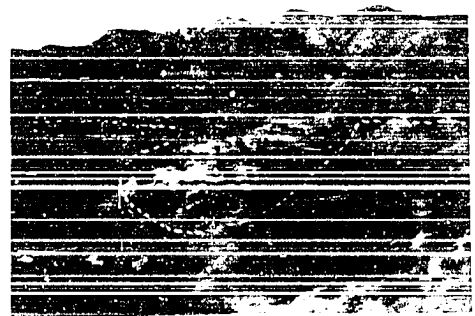
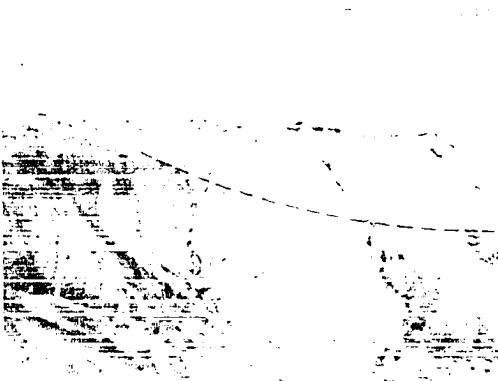
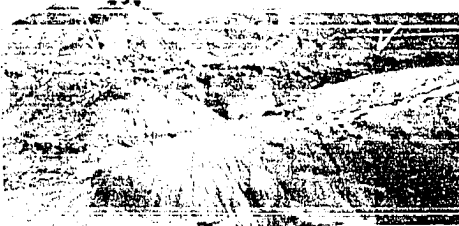
In the central portion of the Basin large lenticular sandstone bodies outcrop which contain a complex association of stratification types including large-scale, epsilon-type cross-bedding (Allen, 1963a) of point bar deposits. Lateral dimensions along an irregular scour surface cut into underlying mudstones range up to approximately 300 yards, while vertical thickness averages 25 feet (Fig. 20a). There is the general absence of a coarse "channel-lag" material in the lower portion of the channel. Upper levels usually display numerous large scale trough and tabular cross-stratification, and horizontal bedding forms as well as localized lenticular out-and-fill sandstone bodies. A systematic vertical variation in sedimentary structures, as reported by Visser (1965), was not observed.

Transitional deposits

Many channel-fills are more restricted in lateral dimension and appear to represent abandonment of a stream channel either through aggradation within an active channel or cut-off during stream meandering. Two general types of

Fig. 20 Photographs of composite structures.

- a. Laterally-extensive channel deposit in central portion of the Big Horn Basin.
- b. U-shaped, sand-filled channel cut into underlying mudstones.
- c. Localized channel sandstone.
- d. Channel fill composed of drab mudstone and truncating subjacent red mudstone.
- e. Channel fill composed of thin, interbedded sandstones and mudstones. Thin sheet sandstone extends laterally from upper portion of channel.
- f. Linear channel sandstone with prominent sheet sandstones extending from the upper portion of the channel.



transitional deposits are recognized. (a) Symmetrical, U-shaped channels cut into mudstones and composed entirely of coarse grained detrital material (Figs. 20b and 20c) are common in the central portion of the Basin. The channel geometry indicates a lack of appreciable lateral shifting during aggradation. The process of in-channel aggradation has been related to a reduction in slope and depth from an extreme sediment supply condition (Allen, 1965), ephemeral stream activity, or restricted flow of sediment-laden waters (Schumm, 1960). (b) Channel-fills derived from active channel abandonment in a meander belt (Figs. 20d and 20e) result either from chute cut-off, in which a new channel is cut into the point bar enclosed by the meander loop, or neck cut-off, resulting from complete abandonment of a loop (Allen, 1965). The Willwood channel in Fig. 20d contains major sandstone bodies in the lower and upper portion and interbedded mudstones (overbank sediments) and thin sandstone lenses in the middle. Such a lithologic assemblage would be deposited in chute cut-off, with the channel undergoing abandonment remaining partially active and periodically receiving an influx of bedload sediment (Allen, 1965). The material filling the channel form in Fig. 20e, predominately a grayish-orange (10YR7/2) mudstone truncating subjacent red mudstones, is characteristic of neck cut-off in which only fine grained sediment is delivered to the abandoned channel during overbank flow.

Overbank deposits

Overbank deposits include sheet sandstones and floodbasin alluvial material. The sheet sandstones extend laterally from the upper level of the channel-fill (Fig. 20f) for distances ranging up to approximately 500 feet. Unit thickness ranges from 1 to 2 feet and is relatively uniform laterally. The general geometry and lateral relationships of the sheet sandstones is similar to natural levee deposits developed marginal to an active stream channel. The sandstones commonly contain tubular structures varying in morphology from straight to curved, subvertical burrows 1/8 to 1/2 inch in diameter filled with silt- and clay-size material to larger, essentially straight and vertical burrows ranging up to 1 inch in diameter and filled with concave sand laminae. Fig. 19e illustrates the larger sand-filled burrows, which resemble the "Taenidium" burrows described by Toots (1967), extending downward into a mudstone underlying the sheet sandstone.

Swale-fill deposits occur along the upper contact of a few sandstone units in the form of lenticular, concave deposits of thinly-bedded, argillaceous sandstones. Allen (1965) relates such features to aggradation within swales developed on the accretionary topography of point bar deposits.

Floodbasin deposits, volumetrically the major alluvial sediment in the central portion of the Basin, include variegated mudstones formed by the deposition of suspended fines from stilled floodwaters. Individual beds present a massive

appearance, with vertical color and textural changes generally of a gradational nature. Mudstone coloration is expressed as either one color or irregular patches of two or more colors (mottled pattern) randomly distributed. Evidence of organic activity is abundant (Fig. 19f) and recorded by either worm burrows filled with "structured" mudstone or thin carbonaceous filaments (roots) occurring either singularly or in an intricate network. Abundant plant material in the form of carbonized wood and leaf impressions are preserved in the thin, laterally persistent beds of carbonaceous shale. Carbonate and iron oxide concretionary material is common on weathered mudstone surfaces as both individual nodules and nodular aggregates or encrustations on fossil fragments. Iron oxide pisolites averaging 3 mm. in diameter were detected in a few mottled mudstone units.

Paleocurrent Data

Information from previous studies on the direction of transport of Willwood sediment is limited to a determination of major source areas to the south and west (Hewett, 1928). This is based solely on the great thickness of Willwood conglomerates in these areas. Unsolved problems concerning the paleocurrent system of the Willwood Formation include the basin-wide pattern of stream entrance and exit and the possible contribution of detritus to the Basin from source areas located to the south (Owl Creek Mountains) and east (Big Horn Mountains).

A total of 3003 cross-bedding measurements and 61 channel and trough trends were secured from Willwood exposures. The direction and degree of dip of foresets and the azimuths of channel and large-scale trough axes were measured. Data was obtained by two independent workers from 46 areas throughout the Basin and combined into 23 localities for tabulation purposes. Paleocurrent data, analyzed by the vector mean method of Reiche (1938), is presented in Fig. 21 and includes the azimuth of the resultant (mean) vector ($\bar{\alpha}$) for each locality and its magnitude expressed in percent (L). Greater values of L reflect a greater concentration of readings. The environmental significance of vector magnitudes is limited, however, by its partial dependence on sample size, with localities of smaller sample size displaying higher concentration values. Azimuths of resultant vectors are plotted in Fig. 1.

Analysis of the vector properties indicates a paleocurrent system in which major stream systems delivered sediment to the Basin from western, southern, and eastern source areas. The average azimuth of 355 degrees reflects the dominant paleocurrent of most Willwood streams in the central and northern portion of the Basin. The lack of major regional differences in vector magnitudes may be attributed to the lack of major change in stream hierarchy, such as from relatively straight and parallel streams of low sinuosity to broadly meandering, high sinuosity streams. The paleocurrent data of areas 1, 2, and 3 in conjunction with granular and pebblesize

Fig. 21 Paleocurrent data.

Locality	Location	Number of Readings (n)	Azimuth of Resultant Vector (\bar{x})	Magnitude of Resultant Vector in Percent (L)
1	T45N, R91W	51	301	60.4%
2	T46N, R91W	89	305	54.8%
3	T48N, R92W	65	273	79.5%
4	T47N, R93W	87	292	47.7%
5	T46N, R93W	212	333	55.4%
6	T45N, R95W	68	308	62.0%
7	T48N, R94W	146	329	58.9%
8	T47N, R96W	207	335	45.0%
9	T48N, R96W	123	338	51.4%
10	T48N, R104W	252	039	40.7%
11	T48N, R99W	68	059	48.7%
12	T49N, R99W	137	027	51.3%
13	T49N, R97W	190	012	55.0%
14	T49N, R95W	43	337	56.4%
15	T50N, R93W	110	337	64.5%
16	T50N, R96W	308	338	54.7%
17	T50N, R99W	311	027	63.8%
18	T50N, R100W	98	031	67.5%
19	T51N, R99W	43	031	67.7%
20	T53N, R97W	49	339	92.5%
21	T54N, R99W	126	041	53.3%
22	T52N, R103W	128	056	49.9%
23	T56N, R101W	84	004	84.7%
All Areas		3100	355	41.3%

$\bar{x} = \arctan \left(\frac{\sum_{i=1}^n n_i \sin X_i}{\sum_{i=1}^n n_i \cos X_i} \right)$, where n_i = number of observations in each class; X_i = mid-point azimuth of the i th class interval.

$L = (\kappa/n)100$, where $\kappa = \sqrt{\left(\sum_{i=1}^n n_i \cos X_i \right)^2 + \left(\sum_{i=1}^n n_i \sin X_i \right)^2}$; n = number of observations.

conglomerates exposed in a Willwood outlier in the northwest portion of T45N, R89W, indicate an east or south-east source area in the Big Horn Mountains.

DISCUSSION AND INTERPRETATION

Provenance

Composition

Synthesis of data suggests the presence of two major source rock lithologies: (1) post-Precambrian sedimentary rocks, and (2) Precambrian igneous-metamorphic mineral assemblages.

The influx of detritus derived from uplifted Paleozoic and Mesozoic sedimentary terranes is recorded by both the mixed carbonate and sandstone, pebble and cobble conglomerates cropping out along the Beartooth Mountain front and subordinate amounts of carbonate pebbles in Willwood conglomerates exposed in the southern and southeastern portion of the Basin. Distinctive rock varieties include cobbles of silicified fossil algae (Condonophycus austini) of the Mississippian Madison Formation and intraformational conglomerate clasts of the Cambrian Gallatin Formation. The abundant chert particles (15%) in sandstones in the central portion of the Basin may have been derived from any or all of several possible Paleozoic source rocks, including the Madison, Amsden, or Tensleep Formations.

Recycled particles from sedimentary rocks are also evident in Willwood sediments. Local derivation of the well-rounded metaquartzite pebbles and cobbles of the Willwood Formation from Paleocene Polecat Bench deposits is supported by field relationships and similarity in external appearance (Hewett,

1928). Hewett envisioned the initial primary source as either a westerly Precambrian, metamorphic terrane or Precambrian cores of the Wind River and/or Gros Ventre Mountains located some 60 miles to the southwest. Anomalous well-rounded and highly spherical, common quartz grains are probably recycled from Paleozoic or Mesozoic sandstones. Well-rounded, low-sphericity grains of ultrastable zircon and tourmaline in Willwood sandstone are interpreted as second or possibly third cycle detritus from post-Precambrian sedimentary rocks.

A primary, Precambrian, igneous-metamorphic source material is indicated by both plutonic acidic and intermediate, and schistose-gneissic rock fragments in the conglomerate lithofacies and grains of angular quartz, feldspar, and accessory minerals in sandstones. Granites appear to predominate in the primary detrital fraction of the conglomerates, particularly at higher stratigraphic levels of the Willwood along the Beartooth Mountain front. Acidic plutonic source rocks, either of igneous or recrystallized metamorphic origin, supplied an abundance of angular, common quartz (35%) and potash feldspar (22%) to the margins of the Basin. Accessory mineral components of euhedral, typically igneous mineral varieties (zircon and tourmaline) plus high-rank metamorphic types (angular garnet, staurolite, and kyanite) also support a significant primary Precambrian source terrane for Willwood detritus. Accessory mineral data, indicating a general increase in metamorphic mineral species (particularly garnet) vertically

through the Willwood and into the Tatman Formation, suggests an increase in exposure and erosion of deep-seated metamorphic rocks. Extremely high concentrations of garnet in Tatman sandstones, however, may have been accentuated by selective sorting (placering).

In situ alteration

Environmental modification of bedrock within Willwood source areas may be indirectly examined through regional floral and faunal evidence and basin-fill mineralogy. The flora and fauna of the early Tertiary, Rocky Mountain region indicates the presence of a warm temperate to subtropical climate with heavy seasonal rainfall (Van Houten, 1948). Modern-day regions characterized by similar climatic conditions generally display an intensely weathered regolith (soil) containing a concentration of aluminium and iron oxides plus hydrous aluminium silicates (kaolinite). Climate, however, is only one of several soil-forming factors. Topographic relief, parent material, and time as reflected in rate of erosion can also influence pedological development, creating a regolith which could be much different from one resulting solely from the climatic factor.

Unstable mineral species, notably feldspars, commonly reflect the intensity of weathering at the source area. Todd and Monroe (1968), on the basis of the presence of kaolinite matrix material and kaolinitic alteration of feldspar varieties in the middle Eocene Domingian sandstones of California.

postulated the presence of an upland source terrane under subtropical climatic conditions of heavy non-seasonal rainfall and lateritic weathering. The unaltered nature of most Willwood feldspar grains indicates the absence of widespread lateritic weathering in the source area. Occasional evidence of incipient, sericitic alteration may be related to soil development, but of a less intense nature.

The clay mineralogy of marginal Willwood mudstones is one of illite dominance accompanied by abundant montmorillinite and subordinate kaolinite. Although the reliability of clay minerals as environmental indicators of source rock alteration is somewhat diluted by evidence of their degradation within fluvial and subaerial environments (Weaver, 1958), many workers (Milne and Earley, 1958) have demonstrated a strong reflection of source material within derived clay minerals, particularly in areas of rapid deposition. The absence of consistent variation in the clay mineralogy of red, purple, and drab mudstones (Fig. 16) suggests a lack of appreciable in situ alteration at the site of deposition. Therefore Willwood clay minerals are largely detrital, derived from adjoining upland source areas.

The minor amount of kaolinite lends support to the postulate that lateritic weathering was not dominant in the Willwood source area. Illite and montmorillinite are commonly associated with pedological environments permitting potassium, magnesium, and calcium ions to remain in the weathered profile

(Grim, 1953). They also predominate in soils developed upon sedimentary rocks because silicate breakdown and lateritic weathering are inhibited by the presence of calcium ions. Paleozoic strata in the region are volumetrically dominated by carbonates, thus providing, in addition to parent material, a prominent source of calcium and sodium ions favoring montmorillinite formation over kaolinite. Drainage conditions within the source terrane, which reflect topography, can also influence the intensity of alteration. Mohr and Van Baren (1954) report the simultaneous development of both "laterite" (kaolinite) and montmorillinite minerals in close proximity from the same parent material and climate. They propose that local areas of improved drainage (increased relief) and removal of ions liberated from parent material were responsible for the increased intensity of silicate breakdown and kaolinite formation.

In situ alteration in the upland Willwood source area was, therefore, not characterized by extensive leaching conditions and rapid breakdown of primary silicates indicative of lateritic soil development. Pedological modification of bedrock was more analogous to soils of the red-yellow Mediterranean type. These soils, found in areas of semihumid climates under a deciduous forest or shrub vegetation, are characterized by (Bennema, 1963): (a) predominance of 2:1 lattice clay minerals (illite and montmorillinite) over 1:1 lattice clay minerals (kaolinite); (b) medium to high concentration of alkalies;

(3) red to brownish yellow B horizons, depending on drainage conditions; (4) an abundance of primary weatherable minerals; and (5) parent material varying from acid to basic. Such a soil appears to more accurately depict the nature of bedrock weathering and pedological development in Willwood source areas.

Origin of the iron oxide responsible for pigmentation of the variegated Willwood mudstones is controversial. For many years reports (Kyrine, 1949; Van Houten, 1948, 1961) have favored red upland soils as the source of the red bed coloring pigment (hematite). Recently Walker (1967a, 1967b) has questioned this hypothesis by demonstrating the development of hematite at the site of deposition through intrastratal alteration of iron-bearing detrital grains and the paucity of modern red sediments in regions presently containing red soils in sediment source areas. This study was unable to establish if the iron oxide pigmenting material in Willwood mudstones was derived from weathered bedrock in the upland source areas or alteration processes in the basin of sediment accumulation. Van Houten (1968) has stated that there may be no truly reliable way to determine the ultimate source of hematite pigment in red beds. It will be demonstrated in the following section, however, that final sediment color is dependent on oxidizing (red) versus reducing (drab) conditions at the site of deposition.

Basin of Deposition

The Willwood Formation consists of two distinct lithofacies which represent three characteristic environmental associations: (1) alluvial fan environment; (2) stream channel and transitional environments; and (3) floodbasin environment. These can be differentiated in the field by both stratigraphic relationships and sedimentological characteristics.

The development of extensive, coalescing alluvial fans along the west flank of the Big Horn Basin is recorded by the conglomerate lithofacies. Conglomerates at lower stratigraphic levels along the Beartooth Mountain front (sec. A-A', Fig. 6) are characterized by the lack of well developed stratification and cross-stratification and overbank mudstones. The absence of these features, along with the abundance of coarse carbonate and sandstone detritus, indicate rapid erosion, transportation, and deposition of material derived from a nearby sedimentary source. Streams draining the east flank of the Beartooths were of a high energy, overloaded and ephemeral nature, with stream- and sheetflooding, sudden gradient decreases, and rapid run-off infiltration common. Movement along fault planes developed at the eastern edge of the Beartooth Mountains may have accentuated these processes.

The metaquartzite cobble conglomerates of the Willwood Formation near Mesteetse and west of Winchester display a less rapid environment of sediment accumulation. The general absence

of fine-grained overbank material and the coarseness of the conglomerates suggest deposition on an alluvial fan. Well developed stratification and large scale cross-stratification, channeling, and interbedded, lenticular sandstones and conglomerates are characteristic of a distributary system of braided streams in the lower reaches of an alluvial fan (Blissenbach, 1954; Allen, 1965). Moderate stream- and sheetflood activity, characterized by well developed sorting and stratification, occurred at greater distances from upland source areas on a piedmont plain formed by the coalescence of several alluvial fans.

Willwood conglomerates grade basinward into a complex association of stream channel, transitional, and overbank deposits. Stream channel and transitional deposits include: (1) a channel complex of sandstone deposits with primary structures indicative of in-channel aggradation and lateral point bar migration; (2) localized fine-grained and fine to coarse-grained channel fills resulting from meander neck and meander chute cut-off or in-channel aggradation; (3) Swale-fill deposits associated with point bar migration and high water (bankfull) conditions; and (4) tabular, thin sheet sandstones (natural levee) resulting from overbank flow.

Synthesis of the above suggests that Willwood streams were predominately of a low gradient, meandering nature. Fluctuations in discharge and load, which would be expected in a climate of heavy seasonal rainfall (Van Houten, 1948).

periodically altered stream activity. Decreased discharge and increased load caused rapid aggradation of active channels and development of localized, U-shaped sand bodies. High stream discharge and overbank deposition of bedload material produced sheet sandstones marginal to channels. The predominance of overbank mudstones (75%) within the sandstone-mudstone lithofacies has been related to prolonged stream confinement within a meander belt (Allen and Friend, 1968). They postulate that the development of appreciable alluvial relief within and marginal (natural levee) to the confined stream system ultimately causes avulsion or the rapid abandonment of a meander belt to a lower level within the floodbasin.

Interchannel areas were the sites of deposition of silt- and clay-size detritus from overbank discharges. Relief across these areas was of an alluvial nature, characterized by a complex pattern of low lying and essentially planar floodbasins adjacent to elevated alluvial ridges of recently abandoned meander belts. Measurements of alluvial relief within similar modern drainage systems vary, with values ranging up to 15 feet (Lorenson and Thronson, 1955). Within the low lying floodbasin areas impeded drainage conditions and water tables at or very near the depositional interface would have favored a reducing environment and preservation of organic matter. Improved drainage and lower water tables in the alluvial ridge and natural levee areas, aided by underlying permeable alluvium, developed oxidizing conditions unfavorable

for the preservation of organic material.

This report, on the basis of the inverse relationship in organic carbon (low-high) to free iron (high-low) and manganese (high-low) in red and drab mudstones (Fig. 17), supports previous studies (Van Houten, 1948; Johnson and Friedman, 1969) proposing a sediment color-depositional environment association of red-oxidizing (well-drained) and drab-reducing (poorly drained) conditions. Such chemical differences result primarily from the increased solubility of ferrous and manganous (reduced) forms leading to solubilization and movement. The greater solubility of reduced manganese over iron may also account for the extremely low values of free manganese in the drab samples examined. The absence of significant variation in aluminium may reflect its lower solubility.

Excluding occasional carbonaceous shales, which represent isolated paludal environments rich in organic material, red and drab mudstones represent "end-member" environments with respect to oxidation and reduction across the aggrading alluvial plain. Between these fall a variety of Willwood sediments accumulating under transitional environmental conditions, causing partial oxidation and/or reduction. Fluctuating ground water tables and climatic factors affecting both vegetation and stream discharge contribute to the complex, multi-colored appearance.

In situ modification processes are also recognized from a pedological or soil genesis aspect. The mudstone sequence

C-12 to C-1 exposed south of the town of Basin displays field properties suggestive of a weathered interval (soil). Intense color mottling (from organic activity), abundant fossil content, and great lateral extent suggest in situ development on a portion of the alluvial plain of a pedologically modified zone during a period of reduced sediment accumulation. Chemical data (Fig. 18) indicates horizons of mobile iron, aluminium, and manganese accumulation. Textural (pipette) analysis also indicates greater amounts of clay-size material in middle to lower portions of the profile. Textural variations could have developed by either depositional ("cumulative" soil of Nikiforoff, 1949) or pedological processes. The independence of free iron and manganese to textural variations, however, indicate that their profile development is related to solution and translocation from upper levels to maxima in the lower levels of the profile. Such mobile ion movement resulted from water table fluctuations causing alternating oxidizing and reducing conditions in the upper portion of the profile, with the deeper movement of manganese a reflection of its greater solubility (de Leon, 1961). The anomalous (low) values of mobile ion constituents in sample C-4 (Fig. 18) may also record an interval of alternating oxidation and reduction in the lower portion of the profile. The presence of an underlying permeable sandstone (sample C-1) could have produced water table fluctuations near the profile base and movement of iron and manganese from unit C-4 to progressively lower levels. The high

correlation ($r = +.735$) between aluminium and clay distribution limits the value of aluminium profile development as an indicator of soil genesis. It should be noted, however, that the higher concentration of clay in the middle portion of the profile may reflect transport of fines to deeper profile levels. If this were the case, clay and aluminium distribution, in addition to iron and manganese, would reflect pedogenesis upon the aggrading Willwood alluvial plain.

Unusually high values of organic carbon in red and purple mudstones indicative of oxidizing conditions supports the contention of extensive organic activity within this mudstone sequence. Van Houten (1948) interpreted similar mottled units to be zones of weathering under moist conditions. Bernard et al. (1962) reported high organic matter in floodbasin deposits displaying mottled and bioturbated soil zones. A fluctuating water table is supported by concretionary calcium carbonate and iron oxide pisolites occurring in many Willwood interchannel mudstones. Analogous features have been reported (Mohr, 1944) in modern-day soils characterized by ground water activity in warm, humid climates with periodic dry seasons.

Soil development is thus characterized by organic matter accumulation and rearrangement of mobile sesquioxides within a parent material (alluvium) not in a steady state but rather undergoing a gradual upbuilding process. Rate of sediment accumulation is considered the critical factor for development of a recognizable soil. Regardless of the intensity of soil

forming factors, time must be available for pedological development to proceed to a point of recognition. In situ modification of alluvial material to the extent depicted above may be uncommon throughout the Willwood strata. A similar process, however, may account for the consistency (90%) of purple beds overlying red beds at higher stratigraphic levels (Fig. 7). Purple Willwood mudstones have gained the attention of previous workers (Sinclair and Granger, 1911; Rohrer and Gazin, 1965), who note their unusually great lateral extent. Chemical data for purple mudstones (Fig. 17), when compared to red mudstones, show similar organic carbon values but lower free iron, aluminium, and manganese percentages. Coupled with the stratigraphic relationships, such data indicate the possibility of alteration of red mudstones through sesquioxide mobilization within a predominately oxidizing and low organic matter environment. Such incipient mobilization may reflect a gradual shallowing (rising) of the fluctuating ground water table within the elevated, oxidizing areas. This was caused by progressive deposition and up-building of the adjacent low-lying floodbasins.

Depositional Patterns

The Willwood Formation represents a portion of the Paleogene influx of detritus eroded from peripheral upland regions into the adjacent basin lowlands during the later stages of the Laramide Revolution. The alluvial fan conglomerates grading basinward into channel sandstones and floodbasin

mudstones, together with the regional tectonic setting, represent a piedmont-valley flat, melasse facies (Van Houten, 1969) developed within the Rocky Mountain intermontane system following the principal orogenic activity. The lack of rapid changes in regional flora and fauna within the Basin during early Tertiary times suggests the absence of prominent geographic barriers, with upland erosion and basin filling maintaining moderate regional relief (Van Houten, 1948). Average rate of sediment accumulation, based on 2300 feet of Willwood sediment accumulating during an early Eocene time interval of 6 million years (Funnel, 1964), is one foot per 2600 years. Such a figure compares favorably with one foot per 3000 years for "Wasatch" deposits of southwestern Wyoming (Bradley, 1930).

Vertically through the Willwood progressive changes in certain mineral, textural, and lithological factors occur, reflecting changing geologic conditions. The greater proportion of metamorphic varieties among the heavy minerals at higher stratigraphic levels indicates an increasing availability of Precambrian metamorphic rocks as upland source areas were progressively dissected. Textural data for sandstones within the central portion of the Basin show improved sorting higher in the Formation, indicating a trend toward reduced stream gradients and lower flow regimes. The dominance of red beds over drab beds and carbonaceous shales in the middle and upper portions of the Willwood suggests a progressive shift within

the aggrading lowlands of a reducing to oxidizing environment. Such a change may indicate a gradual climatic shift to a drier climate causing a general lowering of ground water tables and reduction of organic matter production within the areas of overbank sedimentation.

CONCLUSIONS

- (1) The Willwood Formation consists of a complex association of fluviatile facies, including alluvial fan conglomerates and the vertical and lateral accretionary deposits of stream channel, transitional, and floodbasin sediment.
- (2) Conglomerates reflect local source mineralogy. Those near Meeteetse and west of Winchester are dominated by recycled, Paleocene metaquartzite pebbles, while those bordering the Beartooth Mountain front display an abundance of both sedimentary rocks and igneous and metamorphic varieties.
- (3) In situ alteration of Willwood source material in upland areas was characterized primarily by illite and montmorillonite clay mineral genesis. Subordinate kaolinite indicates some laterite weathering. Modern-day soils containing a similar mineralogy to those indicated for the Willwood source area are of the red-yellow Mediterranean type.
- (4) The main detrital mineral of Willwood sandstones is quartz, with lesser amounts of feldspar, metaquartz, and chert. Mudstones are mainly quartz, with illite and montmorillonite dominate among the clay minerals.
- (5) Sandstones display a variety of simple and composite sedimentary structures reflecting low gradient, meandering streams developing point bar deposits plus chute and neck

out-off features. Fluctuations in stream activity produced local, in-channel aggradation and overbank, (natural levee) deposits.

- (6) The development of alluvial relief by meander belt confinement created drainage and water table conditions favorable for oxidizing (red beds) and reducing (drab beds) environments in interchannel areas.
- (7) Soil genesis upon the Willwood alluvial plain is reflected by the profile development of free iron, manganese, and aluminium within a mudstone sequence.
- (8) Vertical changes in Willwood lithology reflect an increasing supply of Precambrian, metamorphic detritus, lower stream gradients, and a trend toward lower water tables and increasing oxidizing conditions at the site of deposition.

ACKNOWLEDGEMENTS

This report is the result of research supported by National Science Foundation grant GA-1372 awarded to Dr. Carl F. Vondra of the Department of Earth Science at Iowa State University. The writer thanks Dr. Carl Vondra for his supervision throughout all portions of the study. His assistance both in the field and in preparation of the manuscript was valuable to the successful completion of the project. Grateful acknowledgement is given to Professor John Lemish, who reviewed the thesis manuscript. Appreciation is also extended to the staff of the Department of Earth Science for providing helpful suggestions on particular aspects of the study plus facilities and equipment for laboratory work. Special thanks are extended to Messrs. Gary D. Johnson and Steven R. Bredall of the Department of Earth Science, Dr. Roger Q. Landers of the Department of Botany, and Professor Frank F. Riecken, Mr. Harlan L. McKim, and the staff of the Soil Science division of the Department of Agronomy at Iowa State University for their valuable help and advice during various portions of the study.

The writer thanks Messrs. Bruce Bowen, Dennis Powers, John Peckenpaugh, Keith Madsen, Marvin Taylor, and personnel of the vertebrate paleontology division of the Peabody Museum, Yale University for their able assistance in the field. Grateful recognition is also given to the many people of the Big

Horn Basin, whose hospitality and assistance was of great benefit to the successful completion of work in the study area.

Sincere thanks is due my wife, Karen, for both her many hours of manuscript typing and understanding given during the past few years of study.

REFERENCES CITED

- Allen, J. R. L., 1963a, The classification of cross-stratified units, with notes on their origin: *Sedimentology*, v. 2, p. 93-114.
- _____, 1963b, Asymmetrical ripple marks and the origin of water laid cosets of cross-strata: *Liverpool Manchester Geol. Jour.*, v. 3, p. 187-236.
- _____, 1965, A review of the origin and characteristics of recent alluvial sediments: *Sedimentology* (Special Issue), v. 5, p. 89-191.
- Allen, J. R. L., and Friend, P. F., 1968, Deposition of the Catskill facies, Appalachian region; with notes on some other old red sandstone basins: *Geol. Soc. America Special Paper* 106, p. 21-74.
- Andresson, M. J., 1961, Geology and petrology of the Trivoli Sandstone in the Illinois Basin: *Illinois State Geol. Survey Circ.* 316, 31 p.
- Bennema, J., 1963, The red and yellow soils of the tropical and subtropical uplands, p. 72-82 in Drew, J. V. ed., *Selected papers in soil formation and classification*. Soil Sci. Soc. America Special Publ. no. 1, 428 p.
- Bernard, H. A., Le Blanc, R. J., and Major, C. J., 1962, Recent and Pleistocene geology of southeast Texas, P. 177-224 in Rainwater, E. H., and Zingula, R. P., eds., *Geology of the Gulf Coast and central Texas*: *Geol. Soc. America, Guidebook for 1962 Ann. Meeting*, 405 p.
- Blatt, Harvey, and Christie, J. M., 1963, Undulatory extinction in quartz of igneous and metamorphic rocks and its significance in provenance studies of sedimentary rocks: *Jour. Sedimentary Petrology*, v. 33, p. 559-579.
- Blissenbach, Erich, 1954, Geology of alluvial fans in semiarid regions: *Geol. Soc. America Bull.*, v. 65, p. 175-189.
- Bradley, W. H., 1930, The varves and climate of the Green River Epoch: *U.S. Geol. Survey Prof. Paper* 154C, p. 203-223.
- Cope, E. D., 1882, Contributions to the history of the vertebrata of the lower Eocene of Wyoming and New Mexico, made in 1881: *Proc. Am. Philos. Soc.*, v. 20, p. 139-197.
- de Leon, L. V., 1961, Distribution of extractable manganese in some alluvium-derived soils: M. S. thesis, Iowa State University, Ames, 125 p.

- Fisher, C. A., 1906, Geology and water resources of the Big Horn Basin, Wyoming: U.S. Geol. Survey Prof. Paper 53, 72 p.
- Folk, R. L., 1968, Petrology of sedimentary rocks. Austin, Hemphills, 170 p.
- Folk, R. L., and Ward, W. C., 1957, Brazos River Bar: A study in the significance of grain size parameters: Jour. Sedimentary Petrology, v. 27, p. 3-26.
- Funnel, B. M., 1964, The Tertiary period, p. 67-80 in Harland, W. B., Smith, A. G., and Wilcock, Ben, eds., The Phanerozoic time-scale: London, Geol. Soc. London, 276 p.
- Geologic Map of Wyoming, 1955, compiled by Hose, R. K., Love, J. D., and Weitz, J. L.: U.S. Geol. Survey Map MR-3635.
- Gingerich, P. D., 1969, Markov analysis of cyclic alluvial sediments: Jour. Sedimentary Petrology, v. 39, p. 330-332.
- Granger, Walter, 1914, On the names of lower Eocene faunal horizons of Wyoming and New Mexico: Am. Mus. Nat. Hist. Bull., v. 33, p. 201-207.
- Grim, R. E., 1953, Clay mineralogy: New York, McGraw-Hill, 384 p.
- Harms, J. C., and Fahnestock, R. K., 1965, Stratification, bed forms, and flow phenomena (with an example from the Rio Grande), p. 84-115 in Middleton, G. V., ed, Primary sedimentary structures and their hydrodynamic interpretation. Soc. Econ. Paleont. Mineralogists Spec. Publ. no. 12, 265 p.
- Hewett, D. F., 1928, Geology and oil and coal resources of the Oregon basin, Meeteetse, and Grass Creek basin quadrangles, Wyoming: U.S. Geol. Survey Prof. Paper 145, 111 p.
- Holmgren, G. G. S., 1967, A rapid citrate-dichlorite extractable iron procedure: Soil Sci. Soc. America Proc., v. 31, p. 210-211.
- Johnson, K. G., and Friedman, G. M., 1969, The Tully clastic correlatives (Upper Devonian) of New York State: A model for recognition of alluvial, dune (?), tidal, nearshore (bar and lagoon), and offshore sedimentary environments in a tectonic delta complex: Jour. Sedimentary Petrology, v. 39, p. 451-485.

- Kyrine, P. D., 1949, The origin of red beds: N. Y. Acad. Sci. Trans., ser. 2, v. 11, p. 60-68.
- Loomis, F. B., 1907, Origin of the Wasatch deposits: Am. Jour. Sci., 4th Ser., v. 23, p. 356-364.
- Lorens, P. J., and Thronson, R. C., 1955, Geology of the fine-grained alluvial deposits in Sacramento Valley and their relationship to seepage, p. A1-A26 in Banks, H. O., ed., Seepage conditions in Sacramento Valley, Rept. water project authority California.
- McBride, E. F., 1963, A classification of common sandstones: Jour. Sedimentary Petrology, v. 33, p. 664-669.
- McKee, E. D., 1964, Inorganic sedimentary structures, p. 275-295 in Imbrie, J., and Newell, N., eds., Approachs to Paleocology: New York, John Wiley and Sons, Inc., 432 p.
- , 1965, Experiments on ripple lamination, p. 66-83 in Middleton, G. V., ed., Primary sedimentary structures and their hydrodynamic interpretations. Soc. Econ. Paleont. Mineralogists Special Publ. no. 12, 265 p.
- McKee, E. D., and Wier, G. W., 1953, Terminology for stratification and cross-stratification in sedimentary rocks: Geol. Soc. America Bull., v. 64, p. 381-390.
- Middleton, G. V. ed., 1965, Primary sedimentary structures and their hydrodynamic interpretation. Soc. Econ. Paleont. Mineralogists Spec. Publ. no. 12, 265 p.
- Milne, I. H., and Earley, J. W., 1958, Effect of source and environment on clay minerals: Amer. Assoc. Petroleum Geologists, v. 42, p. 328-338.
- Mohr, E. C. J., 1944, The soils of equatorial regions: New York. Edward Bros., Inc., 766 p.
- Mohr, E. C. J., and Van Baren, F. A., 1954, Tropical soils: London, Interscience Publ. Ltd., 483 p.
- Neasham, J. W., and Vondra, C. F., 1967, Stratigraphy of the Willwood Formation, Big Horn County, Wyoming (abs.): Proc. Geol. Soc. America 1967 Annual Meetings, New Orleans, p. 181-182.
- Nikiforoff, C. C., 1949, Weathering and soil evolution: Soil Sci., v. 67, p. 219-230.

- Osborn, H. F., 1909, Cenozoic mammal horizons of western North America: U.S. Geol. Survey Bull. 361, p. 1-90.
- _____, 1929, The titanotheres of ancient Wyoming, Dakota, and Nebraska: U.S. Geol. Survey Mon. 55 (2 vols.), 894 p.
- Peech, M., Dean, L. A., and Reed, J., 1947, Methods of soil analysis for soil fertility investigations: U.S. Dept. Agric. Circ. 757, 432 p.
- Pierce, W. G., 1965, Geologic map of the Deep Lake quadrangle, Park County, Wyoming: U.S. Geol. Survey Map GQ-478.
- Pierce, J. W., and Siegel, F. R., 1969, Quantification in clay Mineral studies of sediments and sedimentary rocks: Jour. Sedimentary Petrology, v. 39, p. 187-193.
- Powers, M. C., 1953, A new roundness scale for sedimentary particles: Jour. Sedimentary Particles, v. 23, p. 117-119.
- Raup, O. G., 1962, Clay mineralogy of the Pennsylvanian red beds and associated rocks flanking the ancestral Front Range of central Colorado: Ph.D. thesis, Univ. Colorado, Boulder, 140 p.
- Reeder, S. W., and McAllister, A. L., 1957, A staining method for the quantitative determination of feldspars in rocks and sands from soils: Canadian Jour. Soil Sci., v. 37, p. 57-59.
- Reiche, Perry, 1938, An analysis of cross-lamination of the Cocconino Sandstone: Jour. Geol., v. 44, p. 905-932.
- Rohrer, W. L., and Gazin, C. L., 1965, Gray Bull and Lysite faunal zones of the Willwood Formation in the Tatman Mountain area, Big Horn Basin, Wyoming: U.S. Geol. Survey Prof. Paper 525-D, p. 133-138.
- Schultz, L. G., 1960, Quantitative X-ray determinations of some aluminous clay minerals in rocks: Seventh Nat'l. Conf. on Clays and Clay Minerals Proc., p. 216-224.
- Schumm, S. A., 1960, The effect of sediment type on the shape and stratification of some modern fluvial deposits: Am. Jour. Sci., v. 258, p. 177-184.
- Shover, E. F., 1964, Clay mineral environmental relationships in Cisco (U. Penn.) clays and shales, north central Texas: Twelfth Nat'l. Conf. on Clays and Clay Minerals Proc., p. 431-443.

- Simons, D. B., Richardson, E. V., and Nordin, C. F., 1965, Sedimentary structures generated by flow in alluvial channels: p. 34-52 in Middleton, G. V., ed., Primary sedimentary structures and their hydrodynamic interpretations. Soc. Econ. Paleont. Mineralogists Spec. Publ., no. 12, 265 p.
- Sinclair, W. J., and Granger, Walter, 1911, Eocene and oligocene of the Wind River and Big Horn Basins: Am. Mus. Nat'l. Hist. Bull., v. 30, p. 83-117.
- _____ and _____ 1912, Notes on the Tertiary deposits of the Big Horn Basin: Am. Mus. Nat'l Hist. Bull., v. 31, p. 57-67.
- Snedecor, G. W., 1956, Statistical methods: Ames, Iowa State University Press, 534 p.
- Todd, T. W., and Monroe, W. A., 1968, Petrology of Domingine Formation (Eocene), at Patrero Hills and Rio Vista, California: Jour. Sedimentary Petrology, v. 38, p. 1024-1039.
- Toots, Henrich, 1967, Invertebrate burrows in the non-marine Miocene of Wyoming: Contributions to Geology Bull., v. 6, p. 93-96.
- Van Houten, F. B., 1944, Stratigraphy of the Willwood and Tatman Formations in northwestern Wyoming: Geol. Soc. America Bull., v. 55, p. 165-210.
- _____ 1945, Review of latest Paleocene and Early Eocene mammalian faunas: Jour. Paleontology, v. 19, p. 421-461.
- _____ 1948, Origin of red-banded Early Cenozoic deposits in Rocky Mountain region: Amer. Assoc. Petroleum Geologists Bull., v. 32, p. 2083-2126.
- _____ 1961, Climatic significance of red beds: p. 89-139 in Narin, A. E., ed., Descriptive Paleoclimatology. New York, Interscience Publishers, Inc., 705 p.
- _____ 1968, Iron oxide in red beds: Geol. Soc. America Bull., v. 79, p. 399-416.
- _____ 1969, Molasse facies: records of worldwide crustal stresses: Science, v. 166, p. 1506-1507.

- Visher, G. S., 1965, Fluvial processes as interpreted from ancient and recent fluvial deposits, p. 116-132 in Middleton, G. V., ed., Primary sedimentary structures and their hydrodynamic interpretations. Soc. Econ. Paleont. Mineralogists Special Publ. no. 12, 265 p.
- Vondra, C. F., 1963, The stratigraphy of the Gering formation in the Wildcat Ridge in western Nebraska: Ph.D. thesis, Univ. Nebraska, Lincoln, 155 p.
- Walker, T. R., 1967a, Formation of red beds in modern and ancient deserts: Geol. Soc. America Bull., v. 78, p. 353-368.
- _____ 1967b, Color of recent sediments in tropical Mexico: a contribution to the origin of red beds: Geol. Soc. America Bull., v. 78, p. 917-920.
- Walkley, A., and Black, T. R., 1934, An examination of the Degtjareff method for determining soil organic matter and a proposed modification of the chromic acid titration method: Soil Sci., v. 37, p. 29-38.
- Weaver, C. E., 1958, Origin and significance of clay minerals in sedimentary rocks: Amer. Assoc. Petroleum Geologist Bull., v. 42, p. 254-271.
- Wolf, K. H., 1965, Gradational sedimentary products of calcareous algae: Sedimentology, v. 5, p. 1-37.
- Wood, H. E. et al., 1941, Nomenclature and correlation of the North American continental Tertiary: Geol. Soc. America Bull., v. 52, p. 1-48.